

<https://doi.org/10.1590/2318-0331.272220220028>

Hydrological-hydrodynamic simulation and analysis of the possible influence of the wind in the extraordinary flood of 1941 in Porto Alegre

Simulação hidrológica-hidrodinâmica e análise da possível influência do vento na extraordinária inundação de 1941 em Porto Alegre

Thais Magalhães Possa¹ , Walter Collischonn¹ , Pedro Frediani Jardim¹  & Fernando Mainardi Fan¹ 

¹Universidade Federal do Rio Grande do Sul, Porto Alegre, RS, Brasil

*E-mails: thaispossa03@gmail.com (TMP), collischonn@iph.ufrgs.br (WC), pedro.fjar@gmail.com (PFJ), fernando.fan@ufrgs.br (FMF)

Received: March 28, 2022 - Revised: September 02, 2022 - Accepted: October 13, 2022

ABSTRACT

The great flood of 1941 remains the most impactful and traumatic flood event in the history of Porto Alegre. This event was caused by a combination of heavy rainfall in the basin in the days prior to the peak of the flood, and the wind that occurred during the flood. However, the influence of wind on the maximum flood level, although frequently mentioned, is not well known. This is largely because there are no systematic data for wind speed measuring and direction in 1941. Therefore, the present work aims to estimate the discharge and the maximum flood level in the city of Porto Alegre and in other relevant points of the basin. using hydrological-hydrodynamic modeling and, from there, analyze the possible role of the wind during the flood, through the simulation of hypothetical wind scenarios. The results showed that the discharges and levels were represented reasonably well with the MGB model at several locations in the basin. In relation to the 1941 event and the scenarios created, the contribution of the wind to the peak of the flood was of the order of a few to tens of centimeters, showing its potential role despite the limitations of the model.

Keywords: Retromodeling; 1941 Great Flood; Porto Alegre; Wind.

RESUMO

A grande cheia de 1941 continua a ser o evento de inundação mais impactante e traumático da história de Porto Alegre. Esse evento foi causado por uma combinação da grande precipitação na bacia nos dias anteriores ao pico da cheia, e do vento ocorrido durante a cheia. Entretanto, a influência do vento sobre o nível máximo da cheia, embora frequentemente mencionado, não é bem conhecida. Isto ocorre em grande parte porque não existem dados sistemáticos de medição de velocidade e direção do vento em 1941. Portanto, o presente trabalho tem como objetivo estimar a vazão e a cota máxima da cheia na cidade de Porto Alegre e em outros pontos relevantes da bacia utilizando a modelagem hidrológica-hidrodinâmica e, a partir daí, analisar o possível papel do vento durante a cheia, através da simulação de cenários hipotéticos de vento. Os resultados mostraram que as vazões e níveis foram representados razoavelmente bem com o modelo MGB em diversos locais da bacia. Em relação ao evento de 1941 e os cenários montados, a contribuição do vento para o pico da cheia foi da ordem de poucos a dezenas de centímetros, evidenciando o potencial papel do mesmo apesar das limitações do modelo.

Palavras-chave: Retromodelagem; Grande Cheia de 1941; Porto Alegre; Vento.



INTRODUCTION

The city of Porto Alegre, capital of the Rio Grande do Sul State, is home to almost 1.5 million inhabitants within the municipal limits and about 4 million inhabitants in the metropolitan region, which is the fifth most populous metropolitan in Brazil. Founded in 1772, the city of Porto Alegre owes much of its grandeur to its privileged location, in a region of confluence between various rivers that drain a total area of over 80,000 km².

At a time when navigation was responsible for almost all the transport of goods and people, this location represented a strategic advantage for the city's port, which allowed access to the production coming from country towns, and to the Atlantic Ocean, through the Patos Lagoon, making the city of Porto Alegre the main commercial center in the extreme south of Brazil.

If, on the one hand, the strategic location at the confluence of several rivers represented a great advantage from an economic point of view, on the other hand, this location also implied losses during flood events. And, among all the flood events that impacted the city of Porto Alegre, the great flood of 1941 is undoubtedly the most relevant.

It is estimated that the flood of 1941 may have flooded 15,000 homes, leaving 70,000 people homeless at a time when the city's population was approximately 272,000 inhabitants (Guimaraens, 2013; Silveira, 2020). The maximum water level during the 1941 flood in Porto Alegre was much higher than the maximum levels of all other recorded floods, both before and after 1941 (Silveira, 2020). But the 1941 flood is not only impressive for the maximum level reached, but also for its long duration, with a third of the affected commercial establishments and industries being flooded for approximately 40 days (Guimaraens, 2013; Silveira, 2020).

Should it happened today, and in the event of the absence or failure of the Porto Alegre flood protection system (built in the 1970s), a flood like the one in 1941 would flood more than 40,000 buildings in the urban area of Porto Alegre in the peak days, and about 20,000 buildings would be affected for more than 30 days, throughout the total duration of the flood (Müller Neto et al., 2019).

The flood of 1941 is not only remarkable in the city of Porto Alegre, but is among the most important, if not the largest, flood event in several places throughout the Patos Lagoon drainage system, such as the cities of Montenegro, São Sebastião do Caí (Fundação Estadual de Planejamento Metropolitano e Regional, 2014), Eldorado do Sul (Fundação Estadual de Planejamento Metropolitano e Regional, 2017) and Rio Grande (Torres, 2012).

For these reasons, the 1941 flood is a traumatic at almost unique event in the history of Rio Grande do Sul, even though the state has a history of disasters that includes droughts (Kulman et al., 2014; Cunha et al., 2019), landslides (Froude & Petley, 2018; Cardozo et al., 2021), extreme winds (Machado & Calliari, 2016; Lima et al., 2020), hail (Nedel et al., 2012; Martins et al., 2017) and frequent floods that can occur practically at any time of the year (Cassalho et al., 2019).

In order to prevent impacts such as those of the 1941 flood from happening again in Porto Alegre, in 1971 it was started the construction of a flood protection system composed of 68 kilometers of levees (6 internal and 5 external), 19 houses of pumps and

various pressurized conduits. Among the external levees there is a concrete wall 3 meters high above the ground located in the central area of Porto Alegre, popularly called “Muro da Mauá”, which has 14 entrances that can be closed with floodgates, and which extends for 2,647 meters along the historic center of the city (Allasia et al., 2015; Müller Neto et al., 2019).

However, since the completion of the flood protection system, no other event has occurred that would justify its construction. This absence of major floods in the recent period has encouraged decision makers to propose changes to the system, with suggestions for resizing and/or replacing fixed protection with mobile structures (Tucci, 1999; Silveira, 2020; G1, 2021; Secretaria de Planejamento, Governança e Gestão do Estado do Rio Grande do Sul, 2021).

Population's progressive forgetfulness of past flood events is not a phenomenon only present in the city of Porto Alegre. As observed by Baldassarre et al. (2013) and Ridolfi et al. (2021), the population of cities affected by riverine floods generally has a relatively short-term memory. According to Fanta et al. (2019), after the occurrence of a flood, the preference for areas far from the rivers increases but, after a few decades, new human settlements emerge again in areas increasingly closer to the rivers, and more subject to riverine floods.

Another factor that seems to motivate the population to believe that an event like the one in 1941 will never happen again is, possibly, a cognitive bias. There seems to be the so-called “wishfull thinking” (Fox-Rogers et al., 2016), or “willingness to believe” in which desires are confused with reality and decisions or reasoning are based on these desires, and not on rationality. This bias seems to motivate the population to believe that certain changes that have taken place in the river basin and in the drainage system, such as the construction of dams, have minimized or even eliminated the chance of a flood similar to that of 1941 from occurring again (Tucci, 1999; Allasia et al., 2015).

The progressive forgetfulness of the flood, and the diffusion of a thought that rules out the possibility of a similar event ever occurring again in the future, may also be related to the scarcity of studies and analysis of this event in the technical literature. Considering the importance of the event at the time it occurred, and its possible impacts if it were to be repeated today, it is surprising that few studies have been carried out on the 1941 flood, its magnitude, and the hydrometeorological processes that led to it, with the exception of the studies by Valenti et al. (2012), Monte et al. (2018), Müller Neto et al. (2019) and Silveira (2020).

This lack of studies and analysis contrasts with what has been suggested in the international technical literature on floods and extreme floods. According to Brazdil & Kundzewicz (2006), really extreme events should be carefully studied even when they occurred in the remote past, prior to systematic data collection. Disastrous historical flood events and their causes should be explored in detail, even when they occurred a long time ago, as their study can be a way of understanding how the event evolved or could have evolved into a disaster. This is because extraordinary floods are often caused by physical processes quite different from those that cause ordinary floods (Merz et al., 2021).

In addition, studies of historical events can be complemented by “if-then” scenarios, through simulation, seeking to identify how

the disaster could be even worse, or how it could be minimized (Merz et al., 2021).

The analysis of individual extraordinary events has become a directive for action in Europe, which suggests that it is important to carry out a description of floods that have occurred in the past and that have had significant adverse impacts on human health, the environment, cultural heritage and economic activity, and for which the likelihood of similar future events is still relevant, including the flooding extent, transport routes and an assessment of the adverse impacts they have entailed (União Europeia, 2007).

This type of deeper analysis of extraordinary hydrological events, through some type of simulation, has been more and more frequently described in the literature, and is called “hydrological reconstruction” (Balasch et al., 2010; Barriendos et al., 2014; Diodato et al., 2019; Vanelli et al., 2020) or “retromodeling” (Remo & Pinter, 2007; Remo et al., 2009), depending on the authors and the techniques used.

“Hydrological reconstruction” or “retromodeling” can be defined as the use of computational methods and modern simulation models combined with available data from the past condition, to estimate values of unknown variables. Eventually this can be done through iterative processes (Remo & Pinter, 2007; Remo et al., 2009; Balasch et al., 2010; Magnuszewski & Moran, 2015; Vanelli et al., 2020; González-Cao et al., 2021). Examples of retromodeling in Brazil were presented by Ribeiro Neto et al. (2015), who analyzed the flood event in June 2010 in the Una river basin (PE), and Vanelli et al. (2020), who analyzed the extraordinary flood of the Tubarão River (SC), which occurred in 1974.

As well as the case study addressed by Vanelli et al. (2020), the flood of 1941 in Porto Alegre can also be considered a composite event, which makes it more complex in relation to retromodeling. Compound events are defined as events resulting from the combination of multiple factors and/or hazards that contribute to social or environmental risk (Zscheischler et al., 2018).

The 1941 flood can be considered a composite event because it was caused by a combination of the precipitation in the basin during the days before the peak of the flood, and the wind that occurred during the flood (Allasia et al., 2015).

Composite events are even more complex to analyze statistically because they result from the interaction between two or more causative variables, whose degree of dependence is not always well known. Therefore, when analyzed from a statistical point of view, events of this type may appear to be outliers. This is the case of the 1941 flood in Porto Alegre, which stands out so much from other flood events that it is, sometimes, considered an outlier (Monte et al., 2018; Silveira, 2020).

In relation to the role of the wind on the system levels, this influence occurs because the Guaíba River and the Patos Lagoon, located downstream, form a very low slope water system, in which the shear stress on the water surface can cause changes in water level, depending on the intensity and direction of the wind (Castelão & Möller Junior, 2003; Cavalcante & Mendes, 2014; Lopes et al., 2018; Tavora et al., 2019). In the Porto Alegre region, the wind blowing over the Patos Lagoon and the Guaíba River can cause increases or decreases in the water level, depending on its direction and intensity. Intense winds blowing from the south quadrant tend to increase the water level at the northern end of

the system, composed by the Laguna dos Patos and the Guaíba River, and intense winds blowing from the north quadrant tend to have the opposite effect.

However, the actual influence of the wind on the maximum level of the 1941 flood in Porto Alegre remains unknown, although frequently mentioned (Guimaraens, 2013; Torres, 2012; Allasia et al., 2015). This is largely because there are no systematic measuring data for wind speed and direction at the time of the great flood.

In this context, the present work presents an application of the MGB model to simulate the great flood of 1941 in the entire watershed of Patos Lagoon, up to its outlet, in the Atlantic Ocean. It is a continuation of the previous work presented by Lopes et al. (2018) and by Martinbianchi et al. (2018), with a special focus on the relative role of rainfall and wind in the formation of the flood peak in the metropolitan region of Porto Alegre. The objective of the work is to assess the possible role of the wind during the 1941 flood, through the simulation of hypothetical wind scenarios, and generate estimates of the flow and the maximum level of the flood in the city of Porto Alegre and in other relevant points of the basin using the hydrological-hydrodynamic modeling adopted approach. At the end, the estimates obtained with the model are compared with estimates from previous works, in local observations and flood marks.

THE PATOS LAGOON WATERSHED AND THE FLOOD OF 1941

Patos Lagoon is a water body with approximately 250 km in length and 40 km in average width, with a surface of more than 10 thousand km² and an average depth of 6 meters (Toldo Junior et al., 2006).

The Patos Lagoon extends in a north-northeast to south-southwest direction parallel to the Atlantic Ocean, from which it is separated by a narrow peninsula. At its southern end, the Patos Lagoon is connected to the Atlantic Ocean by a narrow 22 km long channel, 2 km wide and 12 meters deep, called Barra de Rio Grande. The total drainage area of Patos Lagoon in Barra de Rio Grande is 182,000 km² and includes a part in Brazil (82%) and a part in Uruguay (18%), as shown in Figure 1.

In its southern portion, the Patos Lagoon is connected to the Mirim Lagoon, through the São Gonçalo channel and, through this, to the Manguieira Lagoon. In its northern portion, Patos Lagoon is connected to the Guaíba River, often called Guaíba Lake, on the banks of which the city of Porto Alegre is located.

In the north, Guaíba receives waters from the rivers Jacuí (drainage area of 45,238 km²), Caí (4,983 km²), Sinos (3,694 km²) and Gravataí (2,015 km²), in a region of complex drainage, called Delta do Jacuí, as can be seen in Figure 2. The Jacuí River also receives water from its most important tributary, the Taquari River (26,430 km²), just 42 km upstream from the delta region. The Jacuí, Taquari and Caí rivers drain a mountainous region, with altitudes that reach up to 1000 meters, with predominance of basaltic rocks, which cause a very fast response to rains, in rivers of great declivity. In the vicinity of Guaíba and the metropolitan region of Porto Alegre, however, the relief is flat, the slope is low, occurring extensive floodplains.

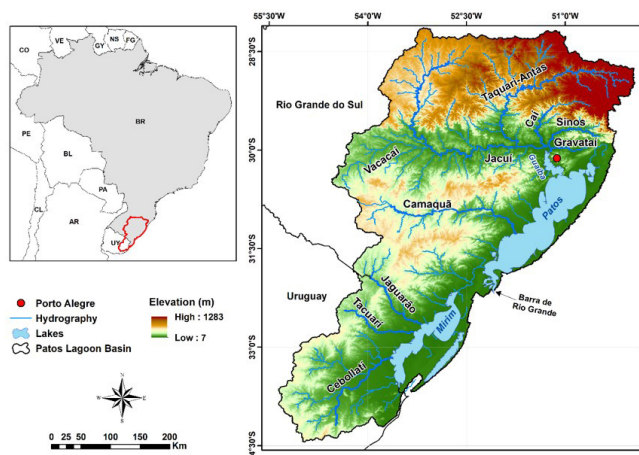


Figure 1. Location of the Patos Lagoon basin and its main tributaries.

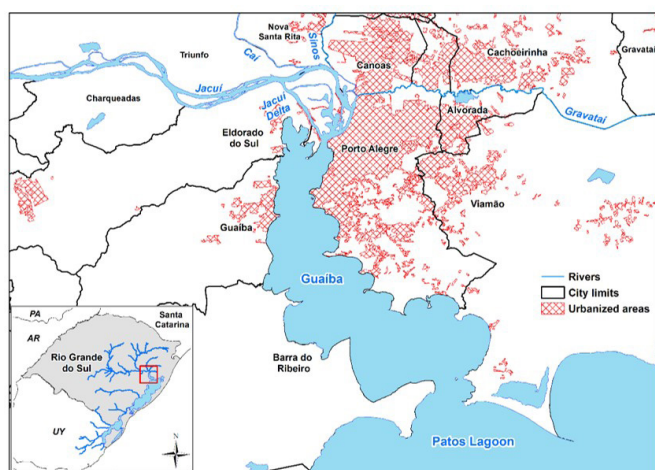


Figure 2. Location of the Jacuí Delta, the main tributaries of the Guaíba and the cities located around the extensive floodplains.

From the Jacuí Delta, upstream, to its connection with Patos Lagoon, at the downstream end, the Guaíba is about 50 km long. The normal surface area of the Guaíba is 470 km², at which the average width is almost 10 km. Guaíba's average depth is approximately 2 m, but there are places with depths of up to 12 m, in its navigation channel, and up to 30 m along Ponta de Itapuã, the region where the connection with Patos Lagoon occurs (Diretoria de Hidrografia e Navegação, 2013).

The ocean influences the Patos Lagoon levels and flow, although the astronomical tidal range of the Atlantic Ocean in the region of Patos Lagoon Barra (known as Barra de Rio Grande) is relatively small, at about 0.50 meters (Möller et al., 2001). Depending on the hydrometeorological conditions, especially the discharge of the rivers that flow into the Lagoon, and the speed and direction of the wind, ocean water enters the Lagoon, reaching regions located up to 180 km upstream Barra de Rio Grande (Antônio et al., 2020).

On the other hand, meteorological tides, known as undertows, which are caused by variations in atmospheric pressure

and wind shear stress on the ocean surface (Pugh, 1987), may have a greater influence on lagoon levels in the proximities of its connection with the ocean. For example, the meteorological tide event that took place in June 2007 at the jetties of Barra de Rio Grande, near the Cassino Beach, caused a rise in sea level of 1.9 m (Parise et al., 2009). At Tramandaí Beach, considering only meteorological and astronomical forces, values greater than 1.2 m above mean sea level were recorded in periods of maximum tidal amplitude (syzygy phase). This even disregarding the effects of rising waves (Andrade et al., 2018).

According to Möller et al. (2001) and Fernandes et al. (2004), low-frequency oscillations (subtidal), associated with meteorological tides and the passage of frontal systems, from 6 to 18 days, are less attenuated at Barra and tend to propagate more in the estuarine part of the lagoon than the high frequency (tidal) oscillations caused by ocean tides. Therefore, the influence of the tides has less importance in the circulation of the Lagoon compared to other factors such as wind and fluvial discharge.

In addition to its influence on the ocean tide near Barra de Rio Grande, the wind acts directly on the Patos Lagoon and on the other water bodies of the water system located on the lowland. This is due to the large size of the system and the coincidence of its longitudinal axis orientation (northeast-southwest) with the prevailing wind direction (Castelão & Möller Junior, 2003; Cavalcante & Mendes, 2014). During most of the year, when the discharges are normally low or moderate, the lagoon circulation is mainly controlled by the wind, unlike when the discharges are higher, as observed at the end of winter, when the tributary flows come to control the circulation of the lagoon (Möller et al., 2001).

According to Castelão & Möller Junior (2003) the water level can vary 8 cm between the extreme north (Itapoã) and extreme south (Ponta da Feitoria) of the lagoon system when winds of 4 m/s (about 15 km/hour) occur, indicating that even greater differences could occur depending on the intensity and direction of the wind. Similar observations were presented in the work by Seiler et al. (2020) (Figure 8 of that article), where it was found that the wind blowing from the southwest quadrant at a speed greater than 8 m/s for 3 days, under low inflow conditions, can cause the water level in the region close to the Guaíba to be about 50 centimeters higher than at the southern end of the lagoon. On the other hand, under winds of the same direction, but with intensities greater than 12 m/s, and in high inflow conditions, this difference reaches 1 meter according to the levels simulated by the numerical model MOHID-2D.

The floods of the Jacuí, Taquari and Caí rivers are formed quickly, in embedded and high-slope rivers, and the response time of these basins is a few days. When they reach the lowland region, still upstream of the metropolitan region of Porto Alegre, the floods start to propagate more slowly, and are attenuated by the presence of extensive floodplains. On the other hand, the Sinos, Gravataí and Vacacaí rivers (a tributary of the Jacuí river from the west) present slower floods.

According to Silveira (2020), the great flood of 1941 started in the middle of April and ended at the end of May. The rains that caused the flood were concentrated in 24 days, from April 13 to May 6, and were widely distributed throughout the watershed.

From the data available on the Hidroweb portal, by the National Water Agency (ANA), the total rainfall over those 24 days was 870 mm in Soledade city, which corresponds to an average daily rainfall of more than 36 mm over almost a month (Silveira, 2020). In cities like Cruz Alta and Santa Maria, the total rainfall values over these 24 days were similar (857 and 829 mm). In Porto Alegre, the rainfall on the same period was 602 mm.

The map in Figure 3 presents the interpolation of total precipitation over the 24 days using the gauges with data at the time and the natural neighbor interpolation method (Smith et al., 2007). It can be observed that the region with the most intense rainfall is the northwest of the basin, which corresponds to the Jacuí River basin, with totals above 800 mm. Rainfall was less intense in the extreme northeast of the basin, which corresponds to the headwaters of the Taquari River, in the extreme south, and along the coast.

The average rainfall accumulated in the Upper Jacuí basin, upstream of the confluence with the Jacuizinho River, reached 691 mm. In the Lower Jacuí basin, upstream of the Taquari outlet, without the contribution of that and Vacacaí, the accumulated precipitation was 593 mm. In the Taquari, Caí, Sinos and Gravataí basins, the accumulated rainfalls were 517, 495, 385 and 370 mm, respectively.

Silveira (2020) states that the total rainfall over the 24 days occurred, to a large extent, during 4 sub-periods, lasting 3 to 6 days each, with intervals of little precipitation between them. Also, according to the same author, the first two sub-periods of rain contributed to saturate the basin soils, which contributed to amplify the response to the precipitation at the last two periods of rain.

Silveira (2020) also mentions that the water level at the Guaíba, before the start of the flood, was relatively low, within the normal expected for the month of April, which would allow

speculating that the same rainy event could result in a flood of even greater magnitude if the basin were in a wetter initial condition.

Maximum flood level in Porto Alegre

Surprisingly, considering the importance of this information, there is considerable uncertainty about the maximum water level reached in the city of Porto Alegre during the 1941 flood.

There are two types of data on the maximum flood level in Porto Alegre in 1941: 1) data from fluviometric gauges; 2) data from historical marks.

According to the only fluviometric gauge with daily data at the time, the Porto Alegre gauge (ANA code 87450000), the Guaíba River reached a maximum level of 4.63 m on May 7. However, the altitude of zero of the ruler of this fluviometric gauge is not known. In addition, some studies point out that the maximum level actually occurred on May 8 (Torres, 2012; Guimaraens, 2013; Valenti et al., 2012; Silveira, 2020).

Even so, the value of 4.63 m is also present in the historical records obtained at the linigraph of Praça da Harmonia gauge, operated by the former federal agency DNPVN (National Department of Ports and Waterways) as presented by Valenti (2010). Another information contained in these records is that the level of 4.63 m was measured following a scale where its level of 3.0 m is equivalent to the height of the deck at Cais do Porto, the city port.

The study carried out by the company Engevix (Brasil, 1968), through the now defunct National Department of Constructions and Sanitation (DNOS), indicates that the peak level would have occurred at 4.75 m. This value presents the same reference level as the linigraph of the old DNPVN and, therefore, differs in 12 cm from the value presented in that one.

The same historical records presented by Valenti (2010), also shows the maximum flood level in Guaíba as 4.62 m, in relation to what was described as the level difference between an existing mark at the central gate of Cais do Porto and the zero of the former Praça da Harmonia gauge ruler which, as well as in the case of the linigraph, registered levels during the flood considering as reference the height of the deck at Cais do Porto. Also, in relation to sea level, the level reached would have been 4.91 m according to the same document.

Among the estimates based on flood marks, we highlight those obtained by Valenti et al. (2012), who estimated the altitude of 4 flood marks from the 1941 event in the city of Porto Alegre. All these measures consider the reference level 1788A of the Brazilian Institute of Geography and Statistics (IBGE), which is tied to the tide gauge of Imbituba. Through this methodology, the authors obtained a value of 4.1621 m above sea level as the peak of the 1941 flood, with a standard deviation of 0.0143 m according to them. The difference found between the 4 flood marks did not exceed 0.034 m. Another value also presented by the authors was 4.6836 m, obtained by relating the estimate of 4.162 m to the current zero of Praça da Harmonia gauge. The value of 4.6836 m was obtained because the IBGE level reference, used to estimate the value of 4.1621 m, is 0.5215 meters above the zero of the ruler currently existing at Praça da Harmonia gauge.

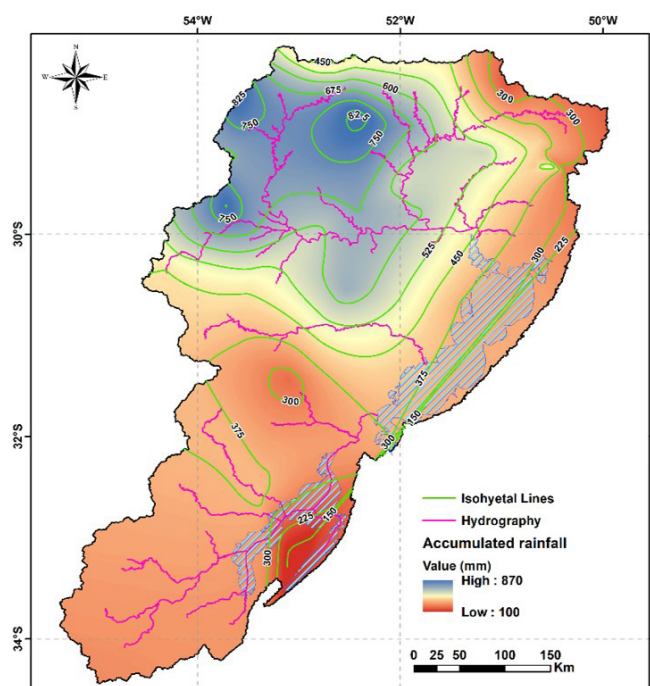


Figure 3. Accumulated precipitation (mm) in 24 days (April 13 to May 6, 1941).

An estimate of the maximum level of the 1941 flood based on a single historical mark was also obtained within the scope of the project translated as “Assessment of the flood protection system of the municipality of Porto Alegre considering the project to revitalize the Cais Mauá” (ABG Engenharia e Meio Ambiente, 2014). The authors of this work measured the altitude of the flood mark, which until today remains on the facade of the Secretary of Treasury of Rio Grande do Sul building, and obtained the value of 4.05 meters (in relation to the tide gauge of Imbituba). The building is located at Mauá Avenue, number 1155, and is located approximately 90 m from Guaíba.

Table 1 presents measurements and estimates of the maximum level reached in the 1941 flood in Porto Alegre and the reference adopted for each of these. The information presented comes from studies carried out in the literature, engineering projects and available data.

In this way, it is clear that there is no consensus for the maximum value of the quota reached in the great flood of 1941 in Porto Alegre. One of the greatest difficulties observed in the works presented is the references used in the estimates and reliability of measurements. Thus, the estimated values are between 4.05 and 4.91 meters, with 4.75 m being the most recurrently mentioned in studies, such as by Valenti et al. (2012), Monte et al. (2018), Müller Neto et al. (2019) and Silveira (2020).

Maximum discharge in Porto Alegre

There are no discharge data measured during the 1941 flood in Porto Alegre. The only estimate of the maximum discharge

of the Guaíba River in Porto Alegre during the 1941 flood was presented by Silveira (2020).

This author estimated a maximum flow of 27,433 m³/s using data from a fluvimetric gauge located in São Jerônimo, on the Jacuí River, located 60 km upstream the city of Porto Alegre. Silveira’s (2020) estimate has considerable uncertainty, because: 1) it was based on data from a fluvimetric gauge far from Porto Alegre; 2) it was based on a large upper extrapolation of a rating curve; 3) was based on the hypothesis of a homogeneous specific maximum discharge, that is, a linear relationship between the drainage area and the maximum flow (which potentially results in an overestimation, since it rained less in the incremental basin, and the incremental basin has different characteristics of the upstream basin).

Maximum discharge in other locations of the basin

In May 1941, 18 fluvimetric gauges were in operation in the basin, and they allow estimating the maximum flow, although the great uncertainty of the rating curve should be highlighted, especially due to the upper extrapolation (Sikorska et al., 2013).

The maximum discharge observed at the gauges is shown in Table 2 and their location in Figure 4. It can be observed that the highest specific discharges were recorded at the gauges Passo Carreiro (86500000), on the Carreiro River, and Santa Lúcia (86580000), on the Guaporé River, both tributaries of the Taquari River.

The highest discharges occurred in the Jacuí River, at the Rio Pardo fluvimetric gauge (85900000), located almost 100 km

Table 1. Maximum levels estimated or measured in the 1941 flood and adopted reference.

Max. Level (m)	Reference level	Method of obtaining	Projects/Literature
4.05	Existing historic mark on the facade of the Treasury Building, referenced to the vertical Datum of Imbituba/SC	Single flood mark	Project “Assessment of the flood protection system of the municipality of Porto Alegre considering the project to revitalize the Cais Mauá” (ABG Engenharia e Meio Ambiente, 2014)
4.1621	Vertical Datum of Imbituba/SC	Multiple flood marks	Estimate by Valenti et al. (2012).
4.62	Difference in level between the existing mark at Cais do Porto and the zero at Praça da Harmonia gauge ruler. Currently, this gauge has a different reference point to that of the time.	Single flood mark	Historical file of the Praça da Harmonia gauge ruler, presented in the work by Valenti et al. (2012).
4.63	Record of the DNPVN linigraph existing at the time, whose zero is 3 m below Cais do Porto.	Ruler measurement	Historical file of the Praça da Harmonia gauge ruler, presented in the work by Valenti et al. (2012).
4.63	-	Ruler measurement	Porto Alegre limnimetric gauge (code 87450000).
4.6836	The 4.162 m level (Valenti et al., 2012) referenced to the current zero of Praça da Harmonia gauge. This zero is 0.5215 m below IBGE’s RN1788A reference.	Multiple flood marks	Estimate by Valenti et al. (2012).
4.75	Record from the DNPVN linigraph existing at the time, whose zero is 3 m below Cais do Porto.	Ruler measurement	Project “Technical and economic feasibility of the defense works of Porto Alegre, Canoas and São Leopoldo against floods” (Brasil, 1968).
4.91	4.62 level summed to 0.29 m. Sea level reference.	Ruler measurement	Historical file of the Praça da Harmonia gauge ruler, presented in the work by Valenti et al. (2012).

Table 2. Maximum discharges observed in fluvimetric gauges in the flood of May 1941 in the Patos Lagoon basin.

Gauge Name	River	Gauge Code	Date	Discharge (m ³ /s)	Specific discharge (m ³ /s/km ²)
Passo Montenegro	Caí	87270000	05/05/1941	767	0.18
Passo Carreiro	Carreiro	86500000	04/30/1941	2083	1.14
Passo do Gabriel	Antas	86100000	05/04/1941	992	0.55
Nova Roma	Antas	86300000	04/30/1941	4600	0.60
Campo Bom	Sinos	87380000	05/06/1941	443	0.15
Linha Colombo	Guaporé	86560000	04/30/1941	1204	0.59
Santa Lúcia	Guaporé	86580000	05/05/1941	2637	1.07
Dona Francisca	Jacuí	85400000	05/05/1941	4984	0.36
Ponte Jacuí	Jacuí	85440000	05/06/1941	8050	0.47
Rio Pardo	Jacuí	85900000	05/07/1941	9185	0.24
Santa Cruz	Pardinho	85850000	05/04/1941	139	0.15
Passo do Meio	Pardo	85780000	05/06/1941	388	0.19
Passo do Prata	Prata	86440000	04/30/1941	2194	0.61
Passo São Sepé	São Sepé	85630000	05/04/1941	244	0.33
Passo Tainhas	Tainhas	86160000	05/04/1941	725	0.65
Muçum	Taquari	86510000	05/05/1941	9836	0.61
Santa Brigida	Vacacaí	85460000	04/27/1941	162	0.22
Passo das Tunas	Vacacaí	85600000	05/05/1941	1535	0.23

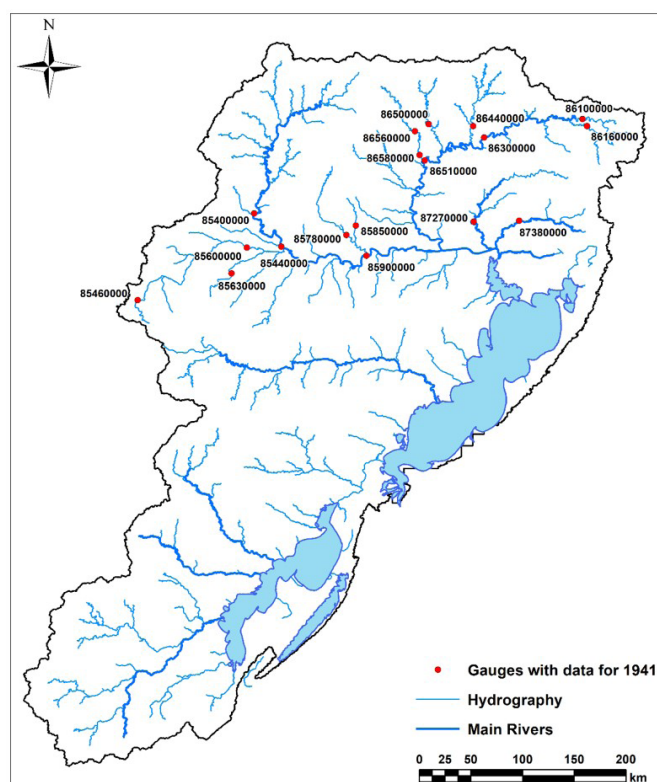


Figure 4. Location of 18 fluvimetric gauges with data during the 1941 flood.

upstream from the confluence with the Taquari river, and in the Taquari River itself, at the Muçum fluvimetric gauge (86510000), located about 150 km upstream the confluence with the Jacuí River. The maximum flow in the Taquari River in Muçum was 9,836 m³/s, and the maximum flow of the Jacuí River was 9,185 m³/s.

Based on these values, it is possible to estimate that the maximum flow at the confluence between these two large

rivers was at the order of 20 thousand m³/s, although the two peaks occurred with a temporal difference of two days, and the contribution in the incremental basin between the fluvimetric gauges and the confluence is not known. In addition, the peak of the flood may have suffered attenuation during the propagation of the flood wave.

METHODOLOGY

In order to estimate the discharge and the maximum level at the Guaíba River, in Porto Alegre, during the extraordinary flood of 1941, and to analyze the possible role of the wind on this same flood, we used a hydrological-hydrodynamic model capable of representing the transformation processes of rain into flow, the propagation of flood waves throughout the Patos Lagoon watershed, and also capable of representing the effect of wind shear stress on water levels. The model chosen was the MGB, in the version initially developed by Lopes et al. (2018), which includes the ability to represent the effect of wind.

The MGB model was initially calibrated in the upper part of the basin, comparing the flow results generated with the flow observations at fluvimetric gauges. In a later step, the parameter of wind shear stress on the water surface was calibrated by comparing water levels time series, calculated at different points of the system formed by Patos Lagoon and Guaíba River, with the levels observed in the same places.

After the two previous calibration steps, the MGB was applied to estimate the maximum discharge and the maximum level of the Guaíba River at Porto Alegre in several hypothetical scenarios with presence or absence of wind, seeking to identify the possible influence of the wind on the maximum levels, even without knowledge of the magnitude and direction of the wind during the 1941 flood.

The calibration of the hydrological model was focused on the most recent period, starting in the 1980s, when there are more observed hydrological and meteorological data. To avoid the

influence of reservoir operation, the discharges calculated by the model in the unit-catchments corresponding to the location of each reservoir (Dona Francisca, Ernestina and Passo Real) were replaced by the respective total outflow from the dams, available on the Reservoirs Monitoring System platform (SAR) from ANA.

Data used

Physical and topological information from the basin was obtained through the DEM of the Shuttle Radar Topography Mission (SRTM), which has a spatial resolution of 3 arcs of a second, approximately 90 m at the equator (Farr et al., 2007). The vertical error of this DEM is less than 16 m and the topography data is available at <http://srtm.csi.cgiar.org> (Jarvis et al., 2008).

The bathymetry of the lagoons and Guaíba was digitized from nautical charts from the Board of Hydrography and Navigation of the Brazilian Navy and inserted into the MDE, enabling the representation of the submerged part of these large water bodies.

Use and soil type characteristics were obtained using the map of Hydrological Response Units (HRUs) prepared by Fan et al. (2015a) for all of South America, through the combination of land use and type maps of different scales.

Meteorological data on temperature, air humidity, atmospheric pressure and insolation were obtained from the MGB's internal database, which presents a set of climatological normals from 1960 to 1990 calculated by the National Institute of Meteorology (INMET) for all the national territory (Fan & Collischonn, 2014). These data were related to each HRU of each unit-catchment, and used in the calculation of evapotranspiration through the Penman-Monteith equation (Shuttleworth, 1993).

Daily data from 487 rainfall gauges (Figure 5a) and 83 pluviometric gauges (Figure 5b) were used in the MGB model, being 22 of the rainfall gauges and 8 of the pluviometric gauges provided by the Uruguay Institute of Meteorology (INUMET - <https://www.inumet.gub.uy/>) and the others by the Hidroweb monitoring platform. During the 1941 flood, only 43 of the pluviometric gauges and 18 of the pluviometric gauges were in operation in the basin, as shown in Figure 5.

Hourly wind speed and direction data from 8 automatic gauges (Figure 6a) from INMET were used in the model to perform the sensitivity analysis of the wind friction coefficient C_D . For this, velocity and direction information were interpolated to the centroid of the closest unit-catchment by the nearest neighbor method. In the case of data failure in all gauges, the influence of the wind for that given date was disregarded.

Data from conventional meteorological gauges, which provide information for every 3 hours, were not used in the simulation because, as shown in the work by Lopes et al. (2018), the levels in Guaíba River are better represented by the MGB model with the inclusion of hourly data of wind. These are obtained from automatic gauges provided by the INMET website.

The wind data set used is available until March 2017 in the vast majority of the gauges, except for Jaguarão, which has data until 2015. The Porto Alegre gauge has the longest period of data (16.53 years), followed by Rio Grande (15.38 years), Camaquã (10.30 years) and Canguçu (10.19 years).

Also, level data from 9 ANA gauges on the Guaíba River and Patos Lagoon were used to evaluate the levels simulated by the model and calibration of the C_D coefficient. The location of the gauges is shown in Figure 6b, as well as each's name. The vast

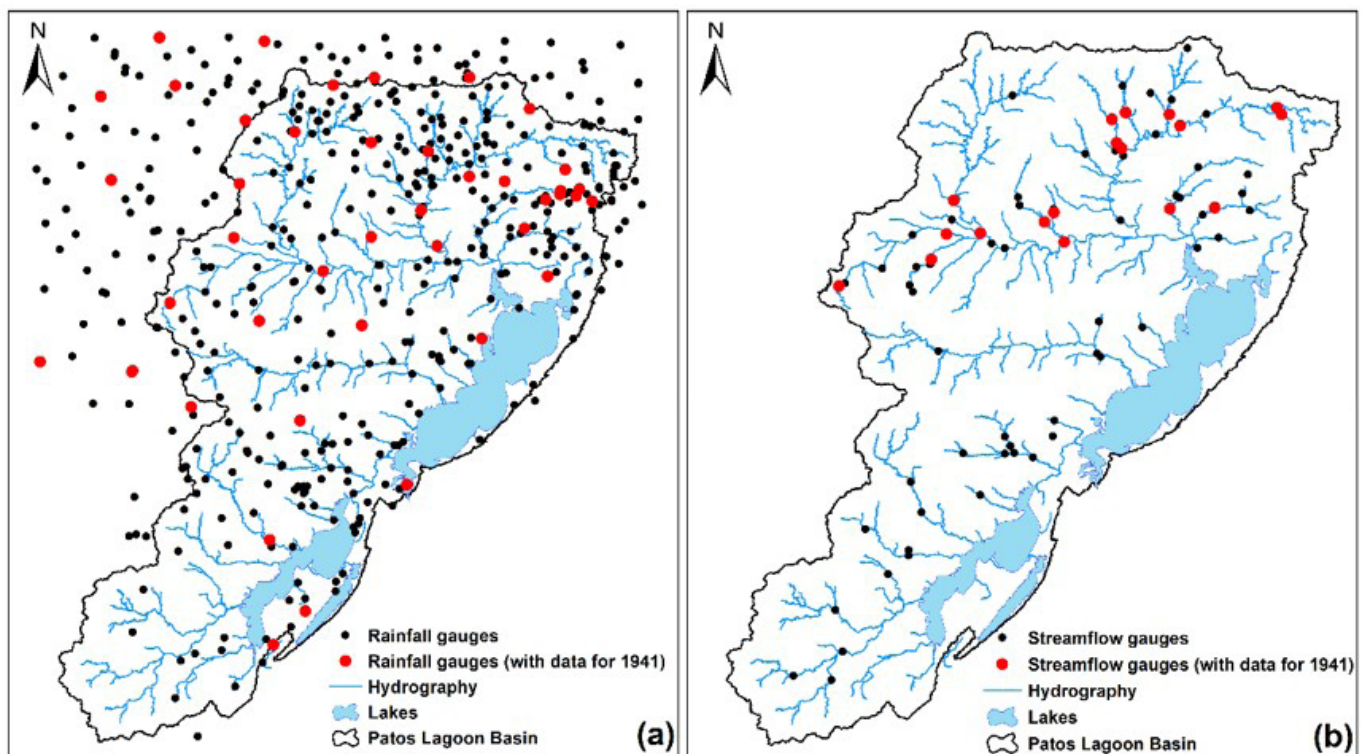


Figure 5. Location of rainfall (a) and fluviometric (b) gauges used in the simulation with the MGB model.

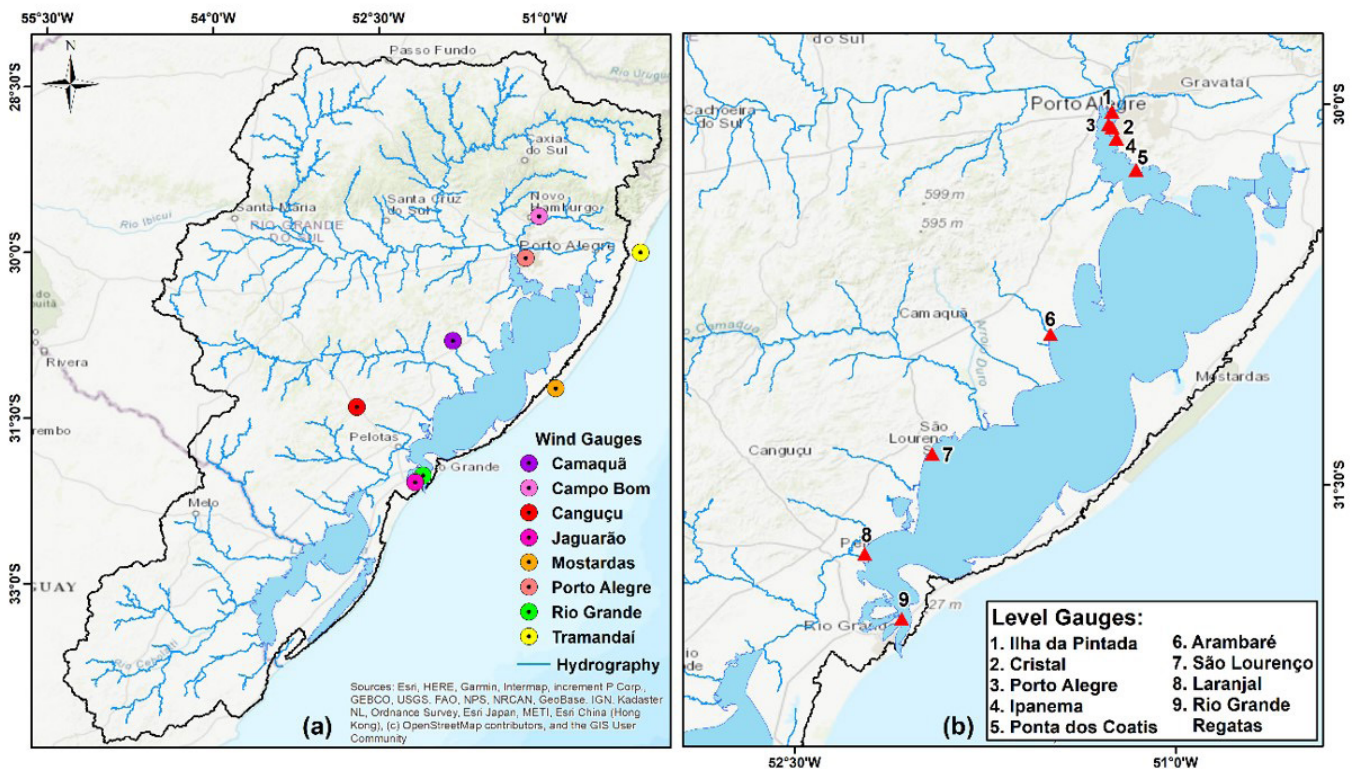


Figure 6. Location of automatic wind (a) and level (b) gauges.

majority of gauges have measurements in the period between 1984 and 2019 and present a reasonable percentage of data in this period, between 41.6% (Ipanema) and 43.1% (Laranjal). The exception is the Porto Alegre gauge, which has information for the period between 1939 and 1952, with only 17% of this interval with actual data. Thus, due to the non-existence data from this gauge in the period with wind information, it was not used to calibrate the wind friction coefficient C_D .

The MGB hydrological model

The MGB model (Large Basins Model) is a semi-distributed, hydrologic-hydrodynamic model that has been widely used in several hydrological studies, including real-time flow forecasting (Fan et al., 2015b; Siqueira et al., 2020), hydrological reanalysis (Wongchuig et al., 2019) and assessment of climate impacts in the Amazon (Sorribas et al., 2016; Almeida et al., 2021).

This model was chosen for this study due to (i) its good performance in simulating South American basins, including the Patos Lagoon basin itself [e.g., Paiva et al. (2011)]; Siqueira et al., 2018; Lopes et al., 2018); (ii) it uses an integrated coupling approach between the hydrological-hydraulic and hydrodynamic models, allowing the representation of backwater effects and the simulation of flat complex basins (Possa et al., 2022); (iii) its use of a simple pseudo-two-dimensional approach that allows complete coupling between simulation models (Pontes et al., 2017) and; (iv) it allows to represent the influence of wind shear on shallow bodies, having been successfully tested by Lopes et al. (2018).

Despite MGB's many advantages, the model also has limitations for application in some basin systems but that, for its use in the present study, do not apply or are not relevant. Such limitations include, for example: (i) considering average values for vegetation parameters (albedo, leaf area index, surface resistance and canopy height) instead of spatially distributed real measurements (Ruhoff et al., 2013); (ii) the inability of the model to represent the process of water uptake by plants, forcing Oliveira et al. (2021) to calibrate different evapotranspiration variables to compensate for this limitation in the Purus River Basin and; (iii) the lower performance in the representation of large basins with semi-arid conditions, like the ones located in Northeast Brazil (e.g., Parnaíba river basin), or also with snowmelt-driven regimes (e.g., Colorado river basin), as this process is not represented by the model (Siqueira et al., 2018).

The model was firstly presented by Collischonn et al. (2007) and has been improved over the last few years by Paiva et al. (2011), Pontes et al. (2017) and Fleischmann et al. (2018). In the latest version of the model, the drainage network is extracted from flow directions obtained from a Digital Elevation Model. The network is then segmented into river stretches of fixed length (Δx) for which small unit-catchments are delimited (Fan et al., 2021). Within each of them, Hydrological Response Units (HRUs) are defined based on soil type and land use.

The model simulates the vertical water balance in each unit-catchment and considers the processes of vegetal interception, evapotranspiration, precipitation, soil infiltration and generation of surface, subsurface and underground runoff. The generated flow in each HRU is directed to the main river channel within

each unit-catchment using linear reservoirs and then propagated along the drainage network.

Within the model, there is an instantaneous exchange of water between river and floodplain, and the surface water elevation is considered the same along the river- floodplain system within each unit-catchment. The river cross sections are represented by a rectangular channel, as commonly assumed in large-scale hydrological models (Paiva et al., 2011; Trigg et al., 2009).

The MGB model has a hydrodynamic calculation methodology for flow propagation in the hydrographic network that solves the Saint-Venant equations expressed by the continuity equations (Equation 1) and momentum conservation (Equation 2) in an almost complete manner, ignoring only the advection, the second term in Equation 2, called inertial method (Bates et al., 2010). It is nonetheless able to represent backwater effects, floodplain attenuation, rivers with low slopes (Pontes et al., 2017; Fleischmann et al., 2018; Possa et al., 2022), or even zero slope, such as the Guaíba River, and other that drain into the Lagos system of the Patos Lagoon basin.

$$\frac{\partial A}{\partial t} + \frac{\partial Q}{\partial x} = 0 \quad (1)$$

$$\frac{\partial Q}{\partial t} + \frac{\partial \left(\frac{Q^2}{A} \right)}{\partial x} + g.A.\frac{\partial h}{\partial x} + g.A.S_f = 0 \quad (2)$$

From these equations, Bates et al. (2010) presents an explicit solution by simple finite differences, where Equation 2 can be rewritten as:

$$Q_i^{t+\Delta t} = \left(\frac{\left(Q_i^t - g.B.\Delta t.(h_{flow_i}.S_{flow_i}) \right)}{\left(1 + \frac{g.\Delta t.h_{flow_i} \cdot \left(\left| Q_i^t \right| n^2 \right)}{B.(h_{flow_i})^3} \right)} \right) \quad (3)$$

Where: Q is the river discharge [m^3/s], A is the flow cross section area [m^2], g is the gravitational acceleration [m/s^2]; Δt is the model time step [s]; x is the distance in the longitudinal direction [m]; h is the flow depth [m]; S_f is the slope from the water surface [m/m]; n is the Manning coefficient; B is the channel width [m]; Q_i^t e $Q_i^{t+\Delta t}$ are the discharges from the unit-catchment i at given times t and $t+\Delta t$ [m^3/s]; h_{flow_i} is the effective flow depth between unit-catchment i and unit-catchment $i+1$ and S_{flow_i} is the water surface slope between unit-catchment i and $i+1$ [m/m] calculated with Equation 4, in which y is the water surface elevation (m/m) and Δx_i is the distance between unit-catchment i and $i+1$ [m].

$$S_{flow_i} = \frac{y_{i+1}^t - y_i^t}{\Delta x_i} \quad (4)$$

The continuity equation (Equation 1) is approximated for each river segment by using Equation 5, where $Q_{in}^{t+\Delta t}$ and $Q_{out}^{t+\Delta t}$ refers to inflow and outflow at the next time step, respectively; $Evqi$ is the evaporation from flooded areas at unit-catchment i [mm]; V

corresponds to the total water stored in the channel and floodplain at unit-catchment i and $Q_{viz}^{t+\Delta t}$ refers to the water exchange between adjacent unit-catchments which are not connected in the river network. The last term allows the pseudo-two-dimensional simulation within floodplain and is calculated by a scheme of lateral connections between unit-catchments.

$$\frac{V_i^{t+\Delta t} - V_i^t}{\Delta t} = \sum Q_{in}^{t+\Delta t} - \sum Q_{out}^{t+\Delta t} - \sum Q_{viz}^{t+\Delta t} - \left(\frac{Evqi.Afl_i}{100} \right) \quad (5)$$

In this scheme, regions are defined that delimit the plain areas in the discretized model and, there, the unit-catchments start to connect to their immediate neighbors through fictitious rectangular channels. Generally, the channels width is established based on local information or through calibration, while the length of the channels is calculated from the sum of the radius of two circles that have areas equivalent to that of the two connected unit-catchments.

This pseudo-two-dimensional approach is like the bifurcation channel flow scheme proposed by Yamazaki et al. (2014) and was initially applied in the MGB model by Pontes et al. (2017) to represent the lateral flow in the floodplains of Bananal Island, followed by Fleischmann et al. (2018) in the Niger River Basin and Lopes et al. (2018) in the Patos Lagoon Basin.

The MGB model adopts an explicit numerical scheme in which, to avoid numerical instability, it must satisfy the Courant-Friedrichs-Levy condition (Bates et al., 2010), which determines the hydrodynamic routing time step, from Equation 6:

$$\Delta t = \alpha \frac{\Delta x}{\sqrt{gh}} \quad (\alpha \leq 1) \quad (6)$$

Where: g is the gravity acceleration [m/s^2]; Δt is the model time-step [s]; Δx is the flow distance [km]; h is the maximum flow depth among all unit-catchments [m] and α is a constant lower than 1, used to avoid numerical instability, with advisable values below 0.9 (Almeida et al., 2021).

Recently, the MGB model was also improved to allow the representation of the wind shear effect on large water surfaces, having been tested in the Patos Lagoon by Lopes et al. (2018). This improved version of the model was also used by Vanelli et al. (2020) in the Tubarão River Basin/SC and Possa et al. (2022) in the Mirim-São Gonçalo.

By including to the wind shear stress (in bold), as presented by Abbott & Price (1994), in the momentum equation of the inertial method (Equation 3), Lopes et al. (2018) obtained the formula given as Equation 7.

$$Q_i^{t+\Delta t} = \frac{\left(Q_i^t - g.B.\Delta t.(h_{flow_i}.S_{flow_i}) + \Delta t.B.C_D.d_{ar}|U|.U.(-\cos(Azvi - Azmi)) \right)}{\left(1 + \frac{g.\Delta t.h_{flow_i} \cdot \left(\left| Q_i^t \right| n^2 \right)}{B.(h_{flow_i})^3} \right)} \quad (7)$$

Where: $Azvi$ is the wind direction (towards where wind originates, hence the negative sign) equivalent azimuth in unit-catchment i ; $Azmi$ is the flow direction azimuth, calculated by an imaginary line that connects centroids of unit-catchment i and $i+1$; U is the wind velocity [m/s]; C_D is the wind friction coefficient [dimensionless]

and d_{ar} is the air density. The term $(-\cos(Az_{vi} - Az_{mi}))$ represents the decomposition of wind velocity in the direction of flow, resulting in values between -1 and 1.

Lopes et al. (2018) simulated the Patos Lagoon basin with and without the inclusion of wind and performed three sensitivity tests: (i) for C_D (Equation 7); (ii) comparison between simulated levels when using hourly or sub-daily (every 3h) wind velocity and direction information; (iii) assessment of the inclusion of tidal effect by inserting level data from Rio Grande Regatas gauge as a downstream boundary condition.

Using a C_D coefficient greater than 10×10^{-6} , as well as hourly wind data, Lopes et al. (2018) obtained the best performance metrics, specially for gauges located at Guaíba. Regarding the inclusion of tidal effect on the results, there was a general improvement at the gauges around 4%, 6% e 2% for Nash-Sutcliffe coefficient (NS), root mean square error (RMSE) and correlation coefficient (R), respectively. The authors emphasize that the measurements at the Rio Grande Regatas gauge introduce not only signals referring to the tide, but also local wind and flow conditions.

As limitations and opportunities for improvement, the authors suggest adopting equations that relate the wind friction coefficient to wind speed and to use different values of this coefficient in different locations in Lagoon and Guaíba river. It is also suggested to explore another approach to define the flow direction inside the Lagoon (Equation 7).

Watershed discretization

The MGB model was applied to the entire defined watershed up to the Patos Lagoon Barra, in Rio Grande. The total area is 180,000 km².

For this study, the adopted value of Δx was 10 km, that is, each segment of river has this length and from this the unit-catchments are delimited in the model. This value was the same successfully used by Fleischmann et al. (2018), Lopes et al. (2018) and Fan et al. (2021).

At Patos Lagoon, Mirim Lagoon and Guaíba River, the discretization followed a slightly different procedure from the conventional one, with the division into regular square unit-catchments interconnected by fictitious channels to represent lateral exchanges, as described by Pontes et al. (2017).

A similar approach was applied by Fleischmann et al. (2020) using the MGB model, where square cells were used to represent the floodplain of the Negro basin, in the Amazon. In this regard, the present work also differs from the one presented by Lopes et al. (2018), in which the unit-catchments in the flooded region had irregular shapes.

For this, straight connection channels were manually traced within the region of the lagoons and perpendicular and parallel limits were vectorized every 10 km, which defined the square mini-basins around these channels. From the established limits for these regular unit-catchments, the flow directions of the cells within them were forced via programming towards the traced channels and, within the cells of these, from upstream to downstream. This allowed the simulation within these regions to be approximated to what would be obtained by a pure 2D model. In this way, the

present work presents a model that could be considered mixed, in which 1D simulation is performed in the portion outside the lagoons and quasi-2D simulation is performed in the lagoons. In Figure 7, it is possible to observe the clear difference between the square unit-catchments in the Guaíba region and in the lagoons in relation to those outside these regions, where the delimitation follows the flow directions obtained from the MDE.

Among the advantages of this new approach proposed in this work, with regular unit-catchments to represent the lagoons, we can mention: simplicity in understanding the model; more reliable representation of reality; possibility of representing flow directions in the lagoon, which would not be possible using irregular unit-catchments and; the standardized definition of the widths in the cells, which is consistent with the size of the cells.

In order to facilitate the calibration step, the basin was further divided into sub-basins, which are considered macro drainage areas constituted by many unit-catchments, where the same set of parameters values are adopted to calibrate the unit-catchments inside each sub-basin. The sub-basins were defined up to the location of the most important fluvimetric gauges and with the largest data series in the basin to adjust the simulated discharges to these locations. The basin discretization process resulted in 28 sub-basins and 2048 unit-catchments (Figure 7).

Regarding the unit-catchments within the lagoons, the width of the lateral link channels was defined as 2.6 km after a series of sensitivity analyzes to find the value that provided the best levels in comparison with the observations from available limnometric gauges. This same value was also adopted as the width of the channels within the unit-catchments that take water from upstream to downstream.

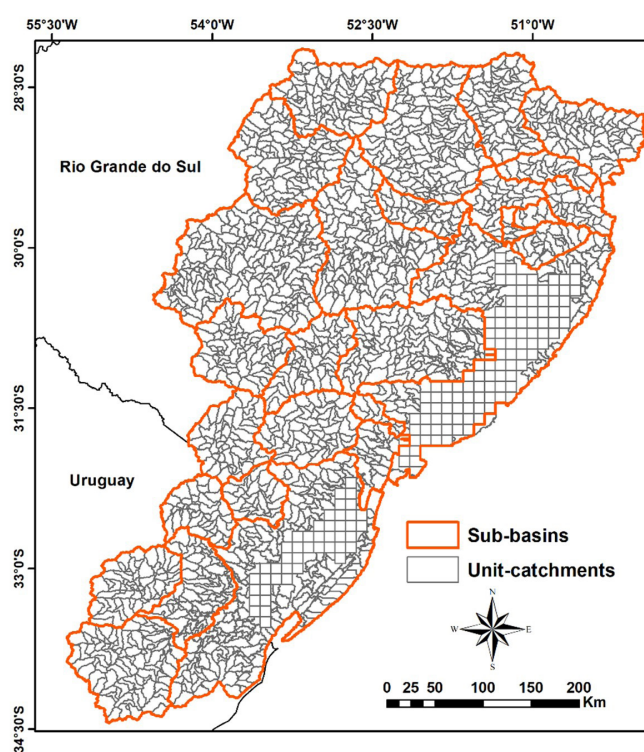


Figure 7. Basin discretization into sub-basins and unit-catchments.

Also through testing, depths of 2.5 m in the Guaíba River and 3.0 m within the lagoon were defined as those that provided best results of simulated levels. Finally, different values of the Manning coefficient were also analyzed, and the one that presented the best results within the lagoons was 0.025. These tests were performed in order to better represent the levels dynamics of the system.

As described, for the application of the model, topological data of the basin (DEM), of precipitation and discharge, of climate (temperature, air humidity, atmospheric pressure and insolation) and the map of HRUs were considered. In addition, a static water level boundary condition was defined at the Patos Lagoon Barra, in Rio Grande, in which a constant level equal to 0.00 meters was assumed. In other words, the effect of astronomical or meteorological tides was not considered.

The choice for not including tide as a downstream condition in the simulation is related to the absence of this information at the time of the 1941 flood or even reports that could serve as basis for the elaboration of different scenarios. Besides, as previously mentioned, there is an attenuation of its effect in Barra de Rio Grande and during the backwater propagation along the estuarine part of the lagoon (Fernandes et al., 2004) being, therefore, less significant in the influence of the levels at upstream portions of the lagoon and Guaíba, specially in a situation of extreme tributary inflow as occur during the flood of 1941.

Calibration of flow-related parameters

Initially, the hydrological model was calibrated to reproduce, in a satisfactory way, the flow hydrographs in 28 fluviometric gauges in several rivers of the Patos Lagoon basin. The calibration of the parameters that control the water balance in the soil and the response speed in the unit-catchments was carried out based on the visual analysis of the observed and simulated hydrographs and evaluation of the objective functions Nash-Sutcliffe coefficient (NS), Nash-Sutcliffe of the logarithms of the discharges (NSlog) and the relative volume error (Bias).

As the representation of the maximum level of the 1941 flood in Porto Alegre is one of the objectives of the work, the performance of the model was also verified when simulating the water levels of Guaíba and Patos Lagoon. To allow comparisons, the level series of the 9 limnimetric gauges located near Guaíba and the lagoon (Figure 5b) had their values adjusted by the difference between observed and simulated averages. In other words, for each location with measurements was calculated the difference between the averages of the simulated and observed series and then the resulting value was subtracted from the complete observed series to place it in the same reference as the simulation. Thus, all series were referenced to the Datum EGM-96, used in the DEM of the SRTM. The model evaluation was performed using the NS performance metrics, root mean square error (RMSE) and correlation coefficient (R) calculated from the simulated levels.

Wind friction coefficient calibration

The C_d aerodynamic friction coefficient controls the intensity of the wind shear effect on the water surface. In the

work by Lopes et al. (2018), the need to carry out sensitivity tests of the C_d parameter is mentioned to better represent the influence of the wind on the levels of Patos Lagoon and Guaíba. Therefore, before analyzing the hypothetical scenarios of different wind characteristics, a sensitivity analysis of the C_d parameter was performed. In these tests, performance metrics NS, R and RMSE were calculated only for the period of greater availability of data from meteorological gauges, therefore, from 2000 to 2017. We evaluated six values for C_d at this stage, all of them within the range mentioned in the literature for the region (Paz et al., 2005; Cavalcante & Mendes, 2014; Lopes et al., 2018; Possa et al., 2022): 10×10^{-6} , 7×10^{-6} , 6×10^{-6} , 5×10^{-6} , 1×10^{-6} , 5×10^{-7} .

Simulation scenarios

Several scenarios were developed to assess how different wind characteristics may have impacted the maximum level of the 1941 flood (Table 3). Combinations of different wind speeds, directions and durations were evaluated to assemble various scenarios and, thus, seek to understand how this force may have presented itself during the event of the maximum level recorded.

To represent different possible intensities, the evaluated values of wind speed were defined according to the Beaufort scale. Each wind speed value was associated with southeast (SE), south (S) and southwest (SW) directions. These directions were chosen because southern quadrant directions can cause an increase in the water level in the region near Guaíba (Seiler et al., 2020). Also, durations varied in 1-day increments, from just the day of the maximum level (08/05/1941), to 7 days in duration, May 2 to May 8 of 1941. It should be noted that the levels simulated in the hypothetical wind scenarios are all referenced to the Datum EGM96, used in the SRTM DEM.

RESULTS AND DISCUSSIONS

This chapter presents the main results obtained during the work carried out. First, the results of the calibration of the MGB model for the Patos Lagoon basin are presented. Subsequently, the simulated levels in the limnimetric gauges found in the Guaíba River and at Patos Lagoon are evaluated. Finally, the results from

Table 3. Simulated wind speed, duration and direction scenarios to assess the influence on the maximum level of the 1941 flood.

Hypothetical wind scenarios	
Velocity [km/h]	Direction [°]
0 (no wind)	-
15	135 (SE)
	180 (S)
	225 (SW)
29	135 (SE)
	180 (S)
	225 (SW)
50	135 (SE)
	180 (S)
	225 (SW)

the different fictitious scenarios of direction, intensity and duration of the wind are also presented.

MGB model calibration results

In order to evaluate the quality of the calibration of the MGB model for the study area, the daily simulated discharges were compared with the observations of 64 fluviometric gauges, with the results for these presented in the form of maps where the spatial distributions and the performance indicators NS, NSlog

and Bias can be visualized (Figure 8). To facilitate the gauges identification and description of the results, different IDs were assigned to the each one, ranging from 1 to 64.

NS and NSlog values were greater than 0.6 in 60% and 68% of the gauges, respectively. It can be seen from the map in Figure 8 that the performance of the model in relation to the NS metric was higher than 0.80 at the gauges located on the Jacuí River (IDs 27 and 28) and Taquari River (IDs 49, 51, 59 and 63). The worst result, but still positive, was observed at gauge with ID 33 (Passo do Meio), belonging to the Pardinho river sub-basin, which presented a NS value equal to 0.23, and NSlog of 0.70. This

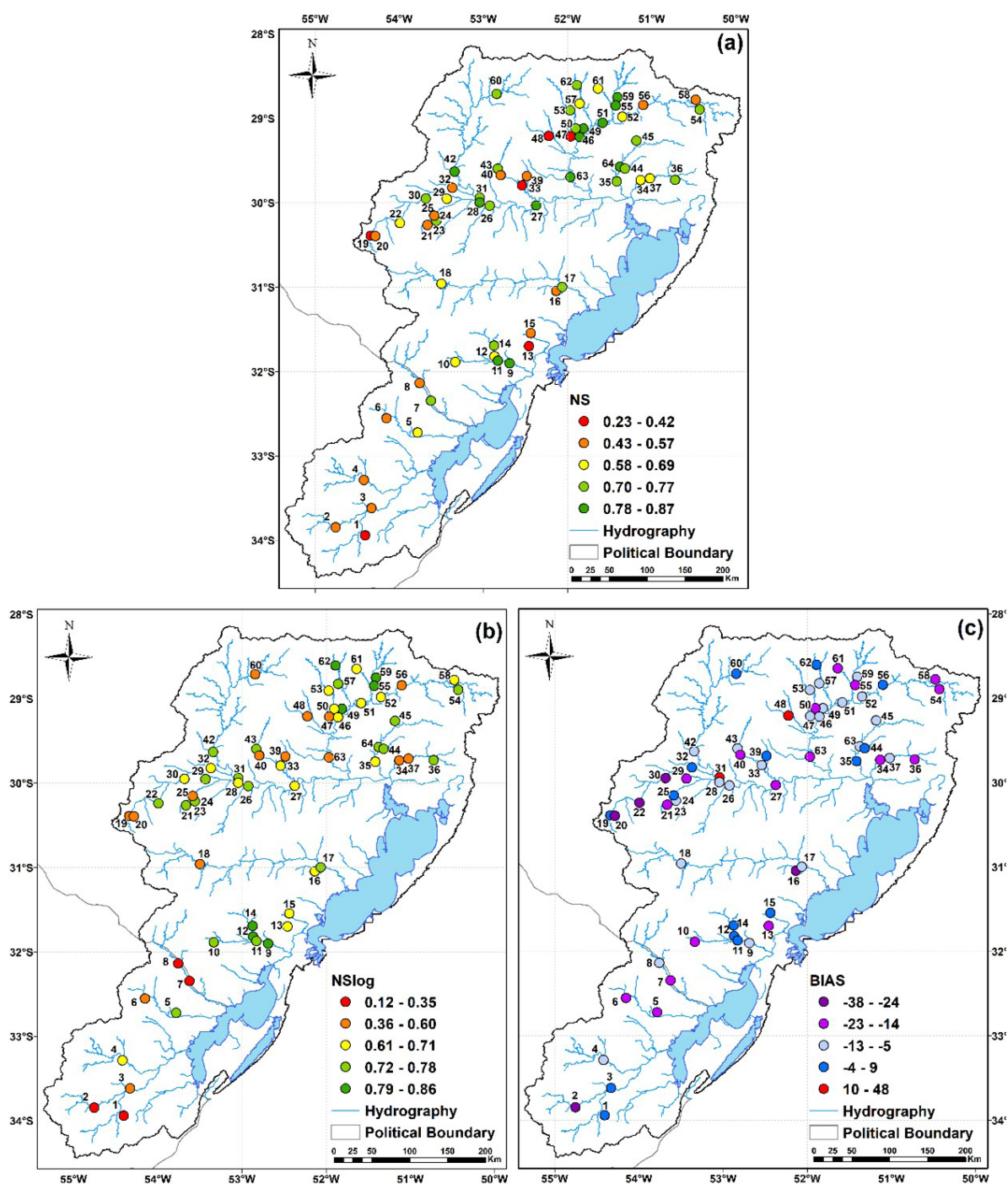


Figure 8. (a) NS, (b) NSlog and (c) BIAS values obtained in the model calibration.

result may be a consequence of the relatively small drainage area (2,070 km²) of the Passo do Meio gauge, its short measurement period (1940-1954), and the low availability of rainfall information in that observed period.

The Uruguayan portion of the basin, bordered by the Atlantic Ocean to the south and Brazil to the north, also proved to be relatively difficult to calibrate, with locations with low proximity between observed and simulated data, as indicated by the NS of 0.28 (ID 1) and NSlog of 0.12 (ID 2). This can be explained by the lack of data from rainfall gauges in the Uruguayan part of the basin during the calibration period.

The NS values indicate a good performance of the model in the representation of peak flows, but there is a tendency to underestimate when analyzing the volumetric error, for which most gauges showed negative values, between -13% and -23%.

In Figure 9 we present some of the hydrographs observed and simulated by the MGB model in the period from 1940's and 1970's, in order to encompass the results for 1941, and also a zoom for that year (right column in the Figure). The main gauges with data for this period are located on the Sinos (37), Caí (35), Antas (52), Taquari (49), and Jacuí (42 and 27) rivers. A visual analysis of the hydrographs shows that, for the entire period presented, the model tends to underestimate the flows at most gauges, with the exception of the Campo Bom gauge on the Sinos River (37)

and Passo Montenegro on the Caí River (35). However, in the 1941 event, the peak flow was underestimated only at the Muçum gauge (49), on the Taquari River.

In the 40's to 70's period, the simulated discharges in the Sinos River reach values of approximately 800 m³/s, while the observations have peaks below 500 m³/s. A similar behavior occurs at the peak of the 1941 flood, in which the simulated was 648 m³/s and the observed 443 m³/s. In this location, there was also a delay of 1 day in relation to the observed. In the Caí River, the simulated peak of 1,605 m³/s, which occurred on the 6th, was 109% higher than the observed, which was 767 m³/s, and had a delay in the peak time of 1 day.

At Passo do Gabriel gauge (52), on the Antas River, the value observed in the event was 992 m³/s and the simulated 939 m³/s, which corresponds to a difference of 5%. The difference in peak timing was 1 day at this location. However, about 127 km downstream, at the Muçum gauge (49), the model obtained a value of 7,434 m³/s compared to the observed of 9,836 m³/s, a difference of 24%. Despite the model underestimate the discharge of the 1941 flood at this location, a good performance was obtained in the full simulation, from 1939's to 1919's, with NS of 0.81. There, the arrival time of the flood wave coincided with that observed, both occurring on May 5th.

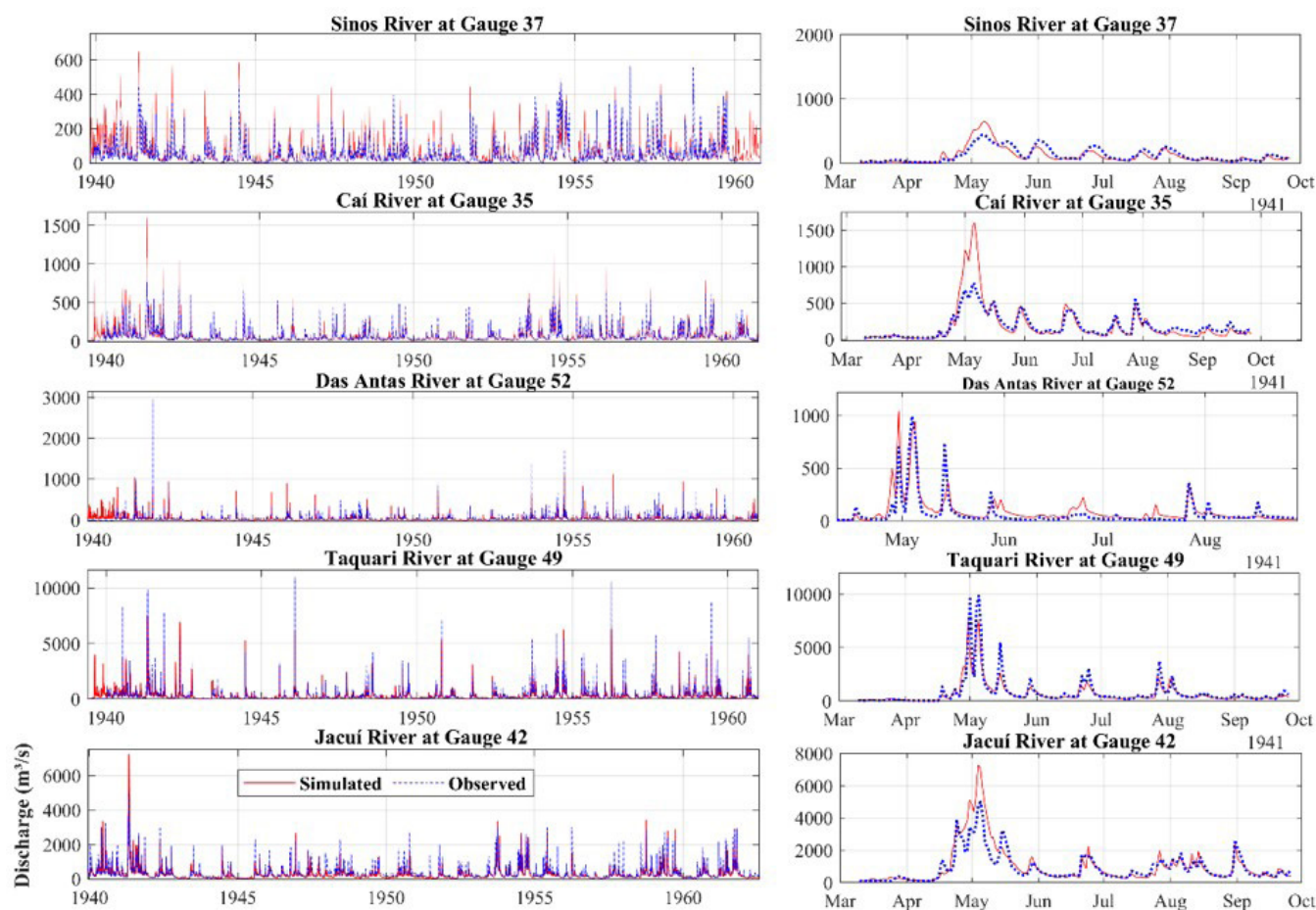


Figure 9. Observed (blue) and simulated (red) hydrographs in the period 1940-1970 (left) and zoomed in 1941 (right) at gauges located in the main tributaries of the basin.

In general, at Dona Francisca (42) and Rio Pardo (27) gauges, both on the Jacuí River, there is a good agreement between the simulated hydrographs and the observed data in the complete simulation, with NS and NSlog of 0.78 and 0.84, respectively. Specifically in the hydrograph of the 1941 flood, at gauge 42 the peak of the simulated discharge, of 7.267 m³/s, did not coincide with the observed of 4.984 m³/s. Still, there was an advance of 1 day on the simulation in relation to the observation, having occurred on May 5th. At gauge 27, further downstream on the Jacuí River, the model adequately represents the magnitude of the peak flow recorded in May 1941, presenting observed and simulated values of 9.185 m³/s and 9.378 m³/s, respectively, however, with a big delay of 4 days in the simulation. If we take specifically the day of the observed peak, on May 7th, the simulated one was 8.123 m³/s, a difference of 12%.

Figure 10 shows the simulated and observed water levels in 9 limnimetric gauges located near the Guaíba river and the lagoon. All gauges are referenced to the EGM96 vertical datum, the same as in the simulation. From the comparison between observed and simulated levels, it is noticed a good representation by the MGB model, mainly in periods of floods. The exception was the Rio Grande Regatas gauge, close to the lagoon's outlet by the sea, where a NS value of 0.20 was obtained. This result is due to the proximity of this gauge to the outlet and the adoption of the downstream boundary condition in the model equal to the constant level of 0 m, that is, without the effect of the astronomical tide and the meteorological tide. This is the same reason why the levels simulated are always above zero meters, which may affect the capacity to better represent negative observed

levels. This could be address in future works by using sea level measurements as boundary condition, but was not consider here as the focus are the maximum levels and because there are no sea level measurements for 1941. For the other gauges, the model obtained NS values ranging from 0.65 in Porto Alegre to 0.73 in Ilha da Pintada, while the R values were between 0.82 in Porto Alegre and 0.87 in Arambaré.

In the observed levels, it can be seen that these oscillations are greater in Rio Grande Regatas and decrease moving upstream in the lagoon, being slightly attenuated in Arambaré. At the simulated levels, these oscillations occur with an amplitude lower than that observed at all gauges, mainly at São Lourenço, Laranjal and Rio Grande Regatas gauges.

In the work by Cavalcante & Mendes (2014), the IPH-A model was used to simulate levels and flows of the lagoon, with a simulation period of 1 year, in 2006, considering the influence of the wind friction coefficient. They also included as boundary condition the flows of the main tributaries of the lagoon, calculated through estimates of the historical series of the limnimetric gauge Ilha da Pintada and fluviometric gauge of the Camaquã river. In this work, the authors obtained NS values lower than those obtained by the MGB model in the present work in São Lourenço and Laranjal. The authors justify the low results in this region due to the effect of the tide and the strong influence of the wind and the applied boundary conditions. It is worth mentioning the short simulation interval of that work.

It is observed that the MGB model had a tendency to underestimate the level in all the analyzed gauges, but it is less evident in the Guaíba levels. In the 2000s, the levels observed

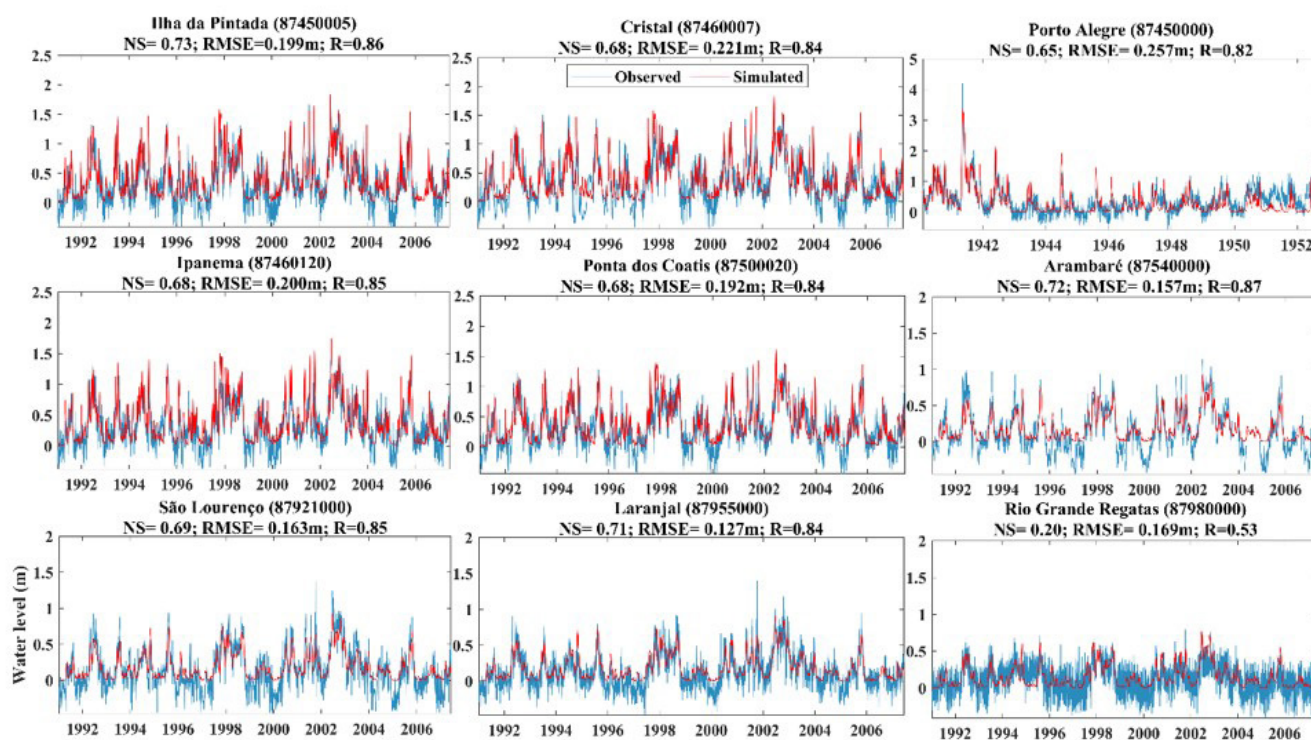


Figure 10. Observed and simulated daily water levels series in Guaíba and Patos Lagoon, referenced to the EGM96 vertical datum, the same as in the simulation.

are higher in Guaíba, with values ranging from 0 to 2 m in Ilha da Pintada and Cristal, in relation to the EGM96 vertical datum. The level decreases as the water moves downstream, towards the Rio Grande Regatas gauge, where levels hardly exceed 1 m. However, even so, at no time did they reach levels as high as observed during the flood of 1941.

During this flood, according to the history data series of the Porto Alegre gauge, Guaíba reached a maximum level of 4.63 m on May 7. On the 8th and 9th of May, levels of 4.40 m and 4.20 m were registered, respectively.

Regarding the outputs of MGB levels, referenced to the EGM96 vertical datum, the peak in Porto Alegre occurred with a delay of approximately 2 days, on May 9, reaching 3.335 m. On the 7th and 8th of May, the model provided levels of 3.219 m and 3.301 m, respectively.

To allow the comparison between observed levels and the series simulated by the MGB, the simulated levels were adjusted to the same reference of the Porto Alegre station. This was done by using the difference between the averages of the two series to dislocate the simulated series. In this particular case, the difference between the simulated and observed averages was 0.505 m, as shown in Table 1. This value was summed to the entire level series generated by the MGB to place it in the same reference as the observed series. Thus, the adjusted peak levels of the simulation were 3.724 m, 3.806 m and 3.84 m for the 7th, 8th and 9th of May, respectively. Therefore, there is a difference of 79 cm between the adjusted simulation and the measurement, considering the maximum level obtained in both series.

By doing the reverse process, using the value of 0.505 m to reduce and bring the observed series to the EGM96 vertical datum, the maximum observed level would be 4.124 m in this reference, as shown in Figure 10.

Compared to the value of 4.05 m (ABG Engenharia e Meio Ambiente, 2014) and 4.1621 m (Valenti et al., 2012), both referenced to the vertical datum of Imbituba/SC, the levels simulated in the present study also show significant differences, between 71.5 and 82.7 cm, respectively. This may be related to the lack of consideration of the wind influence in the event modeling. Therefore, scenarios of possible wind speeds, directions and durations that may have contributed to the increase in the maximum level during the flood were prepared.

As an additional result, the calculation of the difference between the averages of the observed series in relation to the

simulated ones allows to infer what is the difference between the zero of the gauge rulers in relation to the Vertical Datum EGM96, that is, the difference of the zero of the gauges in relation to the sea level. Table 4 presents the observed and simulated averages and the difference between them, which would then be the difference between the zero of the measurement rulers in relation to sea level.

Wind friction coefficient sensitivity analysis

From Tables 5-7, the results of the performance metrics obtained in the sensitivity test to the wind friction coefficient (C_D) are presented, with the best values for each gauge being highlighted in bold. The observed series were also taken to the same reference as the simulation in these comparisons. It can be observed that, with the exception of the Rio Grande Regatas gauge, on average there is a better representation of the simulated levels for the C_D with a value of 5×10^{-6} . Again, the strong influence that the levels observed in the Rio Grande Regatas gauge suffer from the action of the tides is highlighted. For this location, there was even a reduction in the value of the performance metrics with the inclusion of wind, which may be explained by a mismatch in the effect of the simulated wind effects in relation to the oscillations caused by the local tides, which are also influenced by the oceanic winds.

A similar effect can be observed at the Laranjal gauge when the C_D value was different from 1×10^{-6} .

Table 4. Observed and simulated averages and the difference between them.

Gauge	Observed average (m)	Simulated average (m)	Difference (m)
Ilha da Pintada	0.817	0.426	0.392
Cristal	0.837	0.430	0.407
Porto Alegre	0.812	0.307	0.505
Ipanema	0.726	0.415	0.311
Ponta dos Coatis	0.798	0.393	0.405
Arambaré	0.619	0.196	0.423
São Lourenço	0.631	0.195	0.437
Laranjal	0.657	0.189	0.467
Rio Grande Regatas	0.579	0.156	0.423

Table 5. NS values in relation to C_d changes. Best values for each gauge are highlighted in bold.

Gauge	C_d						
	0	10×10^{-6}	7×10^{-6}	6×10^{-6}	5×10^{-6}	1×10^{-6}	5×10^{-7}
Ilha da Pintada	0.734	0.775	0.779	0.777	0.774	0.745	0.740
Cristal	0.659	0.683	0.693	0.693	0.692	0.670	0.664
Ipanema	0.654	0.706	0.711	0.710	0.706	0.670	0.662
Ponta dos Coatis	0.671	0.726	0.731	0.729	0.725	0.688	0.680
Arambaré	0.731	0.804	0.798	0.793	0.787	0.745	0.738
São Lourenço	0.704	0.685	0.723	0.730	0.734	0.717	0.711
Laranjal	0.721	0.371	0.586	0.637	0.678	0.734	0.729
Rio Grande Regatas	0.105	-0.666	-0.308	-0.211	-0.126	0.085	0.095
Average	0.622	0.510	0.589	0.607	0.621	0.632	0.627
Average without Rio Grande Regatas	0.696	0.678	0.717	0.724	0.728	0.710	0.703

Table 6. R values in relation to C_D changes. Best values for each gauge are highlighted in bold.

Gauge	C_D						
	0	10×10^{-6}	7×10^{-6}	6×10^{-6}	5×10^{-6}	1×10^{-6}	5×10^{-7}
Ilha da Pintada	0.870	0.898	0.896	0.895	0.892	0.876	0.873
Cristal	0.843	0.865	0.864	0.863	0.862	0.848	0.846
Ipanema	0.845	0.882	0.878	0.876	0.873	0.853	0.849
Ponta dos Coatis	0.843	0.880	0.877	0.875	0.872	0.851	0.847
Arambaré	0.875	0.905	0.910	0.909	0.907	0.885	0.880
São Lourenço	0.854	0.829	0.857	0.864	0.869	0.864	0.860
Laranjal	0.850	0.717	0.785	0.807	0.826	0.858	0.855
Rio Grande Regatas	0.509	0.322	0.382	0.404	0.426	0.498	0.504
Average	0.811	0.787	0.806	0.812	0.816	0.817	0.814
Average without Rio Grande Regatas	0.854	0.854	0.867	0.87	0.872	0.862	0.859

Table 7. RMSE values in relation to C_D changes. Best values for each gauge are highlighted in bold.

Gauge	C_D						
	0	10×10^{-6}	7×10^{-6}	6×10^{-6}	5×10^{-6}	1×10^{-6}	5×10^{-7}
Ilha da Pintada	0.200	0.184	0.182	0.183	0.184	0.196	0.198
Cristal	0.219	0.211	0.208	0.207	0.208	0.215	0.217
Ipanema	0.201	0.185	0.184	0.184	0.185	0.197	0.199
Ponta dos Coatis	0.193	0.176	0.174	0.175	0.176	0.188	0.190
Arambaré	0.156	0.133	0.135	0.137	0.139	0.152	0.154
São Lourenço	0.158	0.163	0.153	0.151	0.150	0.154	0.156
Laranjal	0.127	0.191	0.155	0.145	0.136	0.124	0.125
Rio Grande Regatas	0.174	0.238	0.211	0.203	0.196	0.176	0.175
Average	0.179	0.185	0.175	0.173	0.172	0.175	0.177
Average without Rio Grande Regatas	0.179	0.178	0.170	0.169	0.168	0.175	0.177

For the other gauges, when comparing the results obtained with the use of this $5 \times 10^{-6} C_D$ in relation to the results of the model without wind ($C_D = 0$), there were average improvements of 4.6%, 2.1% and 6.14% in the NS, R and RMSE metrics, respectively. However, for the limnimetric gauges located in Guaíba, the best NS results occurred when the C_D of 7×10^{-6} was used, and of 10×10^{-6} for the R. Varied results were found for the RMSE metric in these gauges.

Although some specific C_D values were better for the gauges in Guaíba, the difference in the metrics is very small in relation to the simulation with wind considering C_D equal to 5×10^{-6} which, as observed, brings a better general improvement of the representation of the entire system, including the lagoon gauges. When C_D was equal to 7×10^{-6} , NS values of 0.78 were obtained at Ilha da Pintada gauge and 0.73 at Ponta dos Coatis gauge, while, for a C_D of 5×10^{-6} , values close to 0.77 and 0.72 were found, respectively.

Figure 11 shows the observed and simulated water levels at Ilha da Pintada gauge, considering the C_D values for which the best performance measures were obtained at that location, and also the simulation without wind to allow comparison. In this case, the gauge reference was maintained and the simulated series was adjusted to allow comparison. The analysis of the figure shows that the inclusion of the wind effect improved the representation of high frequency oscillations present in the observed data. It can be seen that, by not including this forcing ($C_D = 0$), the oscillations in the simulated results cease to exist, thus indicating the existence of the effects of this variable on the observed levels.

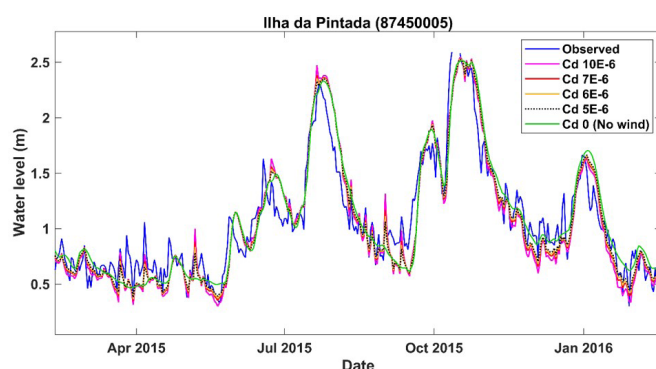


Figure 11. Observed and simulated water levels on Ilha da Pintada gauge considering different values of C_D . The reference in this case is that of the Ilha da Pintada gauge.

In Figure 11, it is also possible to observe that the level oscillations increase proportionally with the wind friction coefficient, in agreement with the results of previous studies carried out in the same region [e.g., Cavalcante & Mendes (2014); Lopes et al. (2018); Possa et al, (2022)]. In the work by Lopes et al. (2018) the optimal C_D value of 10×10^{-6} was found from sensitivity tests. In other studies, such as Cavalcante & Mendes (2014) and Paz et al. (2005), the value of 2.5×10^{-6} was adopted. Both simulated with the hydrodynamic model IPH-A, the first being in Patos Lagoon and the second only in Guaíba. In this work, it was observed that

the value of 5×10^{-6} better represented the simulated levels in the system as a whole, with little difference for the value of 7×10^{-6} , which presented better metrics in the surroundings of Guaíba. Thus, in the subsequent tests of hypothetical wind scenarios, the C_D coefficient of 5×10^{-6} was used.

Results of hypothetical wind scenarios during the 1941 flood

In order to understand the magnitude of the flood and the influence of the wind on the levels, the simulated hydrographs in some of the main rivers of the Guaíba basin were firstly observed. Figure 12 presents the simulation results for the Jacuí River, before and after the Rio Taquari outlet, at the Taquari outlet itself and at the entrance to Guaíba.

It can be noted that the model provides a discharge of $10,192 \text{ m}^3/\text{s}$ in the Jacuí River, before the Taquari River outlet. There, the peak took place on May 13, 7 days before the peak at Taquari outlet, where the peak discharge was $9,079 \text{ m}^3/\text{s}$. After confluence with Taquari river, the Jacuí river reached a peak discharge of $15,864 \text{ m}^3/\text{s}$ on May 7, equivalent to about 97% of the simulated flow at the entrance of the Guaíba during the flood, where the peak simulated discharge was $16,353 \text{ m}^3/\text{s}$. Therefore,

this discharge could have been even higher if the Jacuí and Taquari peaks occurred at the same time, potentially exceeding $20,000 \text{ m}^3/\text{s}$.

From these simulated conditions, the wind scenarios analyzed during the 1941 flood include a first scenario without wind, and 36 scenarios with combinations of wind direction, intensity and duration. Three wind intensities were considered (15, 29 and 50 km/hour); three wind directions (South, Southwest, Southeast) and 4 durations (1, 3, 5 and 7 days). The maximum levels of the 1941 flood in Porto Alegre obtained in each of the 37 scenarios are presented in Table 8.

In the scenario in which the influence of the wind was disregarded, that is, in the scenario without wind, the maximum water level in Porto Alegre was 3.33 meters. At the other extreme, in the scenario with a wind of 50 km/hour, blowing from the South direction, for 7 uninterrupted days before the peak of the observed flood, the maximum water level was 4.32 meters. Between these two extremes, there is a difference of almost 1 meter, which demonstrates that the wind can play a non-negligible role in the floods of Porto Alegre, in particular in the great flood of 1941.

Table 8 shows that winds from the South direction have the greatest influence on the maximum water level in Porto Alegre, followed by winds from the Southeast direction. It can also be seen that, in general, the longer the duration of the wind, the greater the maximum flood level in Porto Alegre. However, this effect is less pronounced in lower wind speed scenarios (15 km/hour) and more pronounced in higher wind scenarios (50 km/hour).

A comparison of the values found in the simulation scenarios, presented in Table 8, with the values of maximum water level obtained from flood marks or from systematic monitoring at the time of 1941, presented in Table 1, reveals that the simulated levels are lower than maximum levels observed for the majority of the scenarios.

Taking as an observed value the maximum level of 4.16 meters estimated by Valenti et al. (2012) from 4 marks of the 1941 flood, it is observed that the maximum simulated levels presented in Table 8 are less than 4.16 meters in 35 of the 37 simulated scenarios. Only in south wind conditions, with an intensity of 50 km/hour, and lasting 5 and 7 days, does the maximum simulated level exceed the maximum observed level.

Winds from the South quadrant, with speeds close to 50 km/hour, and lasting for a few days, can occur over Patos

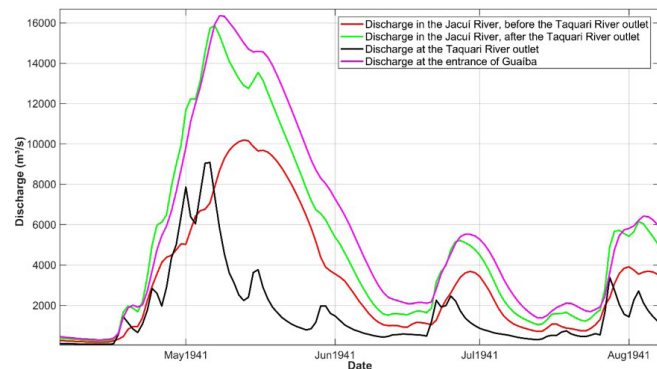


Figure 12. Simulated hydrographs in the Jacuí River, before (black) and after (green) the Taquari river outlet and at the Taquari outlet (red).

Table 8. Results obtained for the hypothetical scenarios of speed, duration and wind direction. The reference is the Vertical Datum EGM96.

Hypothetical wind scenarios		Maximum level (m) for different days of wind duration, until 05/08/1941			
Velocity (km/h)	Direction (°)	Day 08	From day 06 to 08	From day 04 to 08	From day 02 to 08
No wind		3.33			
15	135 (SE)	3.35	3.36	3.36	3.36
	180 (S)	3.36	3.37	3.38	3.38
	225 (SW)	3.34	3.35	3.35	3.35
29	135 (SE)	3.48	3.50	3.51	3.52
	180 (S)	3.51	3.55	3.57	3.59
	225 (SW)	3.42	3.45	3.47	3.50
50	135 (SE)	3.88	3.95	3.98	4.01
	180 (S)	4.00	4.13	4.24	4.32
	225 (SW)	3.69	3.82	3.92	4.00

Lagoon and Guaíba River associated with extratropical cyclones. The occurrence of winds from the South quadrant after a period of heavy rainfall in the Patos Lagoon basin cannot be considered an abnormal combination either. However, a period of 5 to 7 days, with constant wind from the south direction, and, more importantly, with a speed of 50 km/hour, seems to exceed the typical conditions of a cyclone in the region. Furthermore, historical records, while mentioning wind, do not report a duration as long, or as severe an intensity, as this simulated extreme condition.

Unfortunately, there are no records of wind measurements before and during the peak of the flood in the region that would allow checking which of the wind scenarios is more plausible. The search for meteorological reanalysis data reveals that the wind in the period of 7 days before the peak of the flood had variable speed, less than 50 km/hour, and its direction was not constant. In spite of the low reliability of the meteorological reanalysis data in the year 1941, a period before the more systematic data collection, the hypothesis of an important cyclone, with strong and sustained wind for almost a week, along the eastern region of Rio Grande do Sul does not have much support.

In wind scenarios that can be considered more plausible, with winds from the South quadrant with intensities between 29 km/hour and 50 km/hour, and lasting two days, the maximum simulated level is between the values of 3.55 meters and 4.13 meters. These two values are 61 cm and 3 cm lower than the observed mark of 4.16 meters (Valenti et al., 2012), and suggest that the MGB hydrological model may be underestimating the hydrological component of the flood.

In other words, in the simulation described here, the MGB model appears to be underestimating the magnitude of the 1941 flood in Porto Alegre, and the maximum observed level can only be reproduced in an extremely intense wind scenario, which does not seem plausible in view of the reports from witnesses of the event, and meteorological reanalysis data.

The underestimation of the maximum level simulated by the MGB may be related to several causes, including limitations of the model, the input data and the methods for handling the input data. For example, it was observed, preliminarily, that the estimated total precipitation in some important sub-basins for the formation of the flood varies in a relevant way, depending on the interpolation method used to estimate the precipitation in the model's unit-catchments from the data observed in the rainfall gauges.

One factor that may have limited the results is the consideration of a constant level of the Atlantic Ocean, at Barra do Rio Grande, where the downstream boundary condition of the hydrological-hydrodynamic model is defined. A rise in sea level in this region as a result of a meteorological tide (underwater) could contribute to an increase in the flood level.

Another factor that may be contributing to the underestimation of the maximum flood level in Porto Alegre by the MGB is that in the simulated hydrographs there is a greater lag than that observed between the hydrographs of the Jacuí and Taquari rivers. This increase in the lag results in a reduction in the simulated peak flow, in relation to what would occur if the floods of the two rivers were more synchronized and in accord to the dates of the observed data.

In any case, although it was not possible to reproduce exactly the maximum observed level of the flood, the results obtained are important in demonstrating that the wind may have played a relevant role in the flood, possibly contributing with a few centimeters, or even a few tens of centimeters, for the formation of the flood peak in Porto Alegre.

CONCLUSIONS

This study presents the discharges and levels simulated for the extraordinary flood of 1941 in relevant points of the Patos Lagoon basin and in the city of Porto Alegre. For this, hydrological-hydrodynamic modeling was used in a fully coupled 1D and quasi-2D hybrid model (MGB).

In the system formed by Patos Lagoon and Guaíba River, the MGB model satisfactorily reproduced time series of water level observed in the most recent period, even without the influence of tidal effects, which should be further explore in future works.

We concluded that the contribution of the wind to the peak of the flood is on the order of a few centimeters to a few tens of centimeters. In an extreme wind scenario, which seems implausible considering the available information, the wind contribution in the formation of the flood peak could have approached 1 meter.

The 1941 flood retromodeling exercise suggests that the event was underestimated by a few tens of centimeters by the MGB model, which may be related to the limitations of the hydrological model, the input data or the data pre-processing methods, such as the algorithm for spatial interpolation of precipitation from point data at fluvimetric gauges.

There are many uncertainties for the representation of the 1941 flood, such as: extrapolations of the rating curve in the observations; measurement and interpolation of large volumes of precipitation; lack of distributed or consolidated information on levels in Guaíba and Patos Lagoon, and; lack of measured information on wind speed and direction during the event. These uncertainties, as well as the tendency to underestimate the magnitude of the 1941 flood, will be analyzed in subsequent stages of this work.

There are currently many discussions about the need for flood containment systems implemented in Porto Alegre as they were designed, taking into account the 1941 flood. In future works, we intend to use the tool developed to analyze the possible impact on the 1941 flood of several changes that have taken place in the basin since then, including the construction of dams and reservoirs and possible climate changes.

REFERENCES

- Abbott, M. B., & Price, W. A. (1994). *Coastal estuarial and harbour engineer's reference book*. London: E & FN Spon.
- ABG Engenharia e Meio Ambiente. (2014). *Avaliação do sistema de proteção contra cheias do município de Porto Alegre considerando o projeto de revitalização do cais Mauá*. Porto Alegre: ABG Engenharia e Meio Ambiente.

- Allasia, D. G., Tassi, R., Bemfica, D., & Goldenfum, J. A. (2015). Decreasing flood risk perception in Porto Alegre–Brazil and its influence on water resource management decisions. *Proceedings of the International Association of Hydrological Sciences*, 370, 189-192. <http://dx.doi.org/10.5194/piahs-370-189-2015>.
- Almeida, R. M., Fleischmann, A. S., Brêda, J. P., Cardoso, D. S., Angarita, H., Collischonn, W., Forsberg, B., García-Villacorta, R., Hamilton, S. K., Hannam, P. M., Paiva, R., Poff, N. L., Sethi, S. A., Shi, Q., Gomes, C. P., & Flecker, A. S. (2021). Climate change may impair electricity generation and economic viability of future Amazon hydropower. *Global Environmental Change*, 71, 102383. <http://dx.doi.org/10.1016/j.gloenvcha.2021.102383>.
- Andrade, M. M., Toldo, E. E., & Nunes, J. C. R. (2018). Tidal and subtidal oscillations in a shallow water system in southern Brazil. *Brazilian Journal of Oceanography*, 66, 245-254.
- Antônio, M. H. P., Fernandes, E. H., & Muelbert, J. H. (2020). Impact of jetty configuration changes on the hydrodynamics of the subtropical Patos Lagoon estuary, Brazil. *Water*, 12(11), 3197.
- Balash, J. C., Ruiz-Bellet, J. L., Tuset, J., & Oliva, J. M. (2010). Reconstruction of the 1874 Santa Tecla's rainstorm in Western Catalonia (NE Spain) from flood marks and historical accounts. *Natural Hazards and Earth System Sciences*, 10(11), 2317-2325. <http://dx.doi.org/10.5194/nhess-10-2317-2010>.
- Baldassarre, G., Viglione, A., Carr, G., Kuil, L., Salinas, J. L., & Blöschl, G. (2013). Socio-hydrology: conceptualising human-flood interactions. *Hydrology and Earth System Sciences*, 17(8), 3295-3303. <http://dx.doi.org/10.5194/hess-17-3295-2013>.
- Barriendos, M., Ruiz-Bellet, J. L., Tuset, J., Mazón, J., Balash, J. C., Pino, D., & Ayala, J. L. (2014). The “Prediflood” database of historical floods in Catalonia (NE Iberian Peninsula) AD 1035–2013, and its potential applications in flood analysis. *Hydrology and Earth System Sciences*, 18(12), 4807-4823.
- Bates, P. D., Horritt, M. S., & Fewtrell, T. J. (2010). A simple inertial formulation of the shallow water equations for efficient two-dimensional flood inundation modelling. *Journal of Hydrology*, 387(1-2), 33-45. <http://dx.doi.org/10.1016/j.jhydrol.2010.03.027>.
- Brasil. Departamento Nacional de Obras de Saneamento – DNOS. (1968) *Estudo de viabilidade técnico-econômica das obras de defesa de Porto Alegre, Canoas e São Leopoldo contra inundações*. Porto Alegre: DNOS.
- Brazdil, R., & Kundzewicz, Z. W. (2006). Historical hydrology. *Hydrological Sciences Journal*, 51(5), 733-738. <http://dx.doi.org/10.1623/hysj.51.5.733>.
- Cardozo, G. L., Zanandrea, F., Michel, G. P., & Kobiyama, M. (2021). Inventário de movimentos de massa na bacia hidrográfica do rio Mascarada/RS. *Ciência e Natura*, 43(31), 1-26. <http://dx.doi.org/10.5902/2179460X43594>.
- Cassalho, F., Beskow, S., Mello, C. R., Oliveira, L. F., & Aguiar, M. S. (2019). Evaluation of flood timing and regularity over hydrological regionalization in Southern Brazil. *Journal of Hydrologic Engineering*, 24(8), 05019022. [http://dx.doi.org/10.1061/\(ASCE\)HE.1943-5584.0001815](http://dx.doi.org/10.1061/(ASCE)HE.1943-5584.0001815).
- Castelão, R. M., & Möller Junior, O. O. (2003). Sobre a circulação tridimensional forçada por ventos na Patos Lagoon. *Atlântica*, 25(2), 91-106. Retrieved in 2022, February 18, from <http://repositorio.furg.br/handle/1/2866>
- Cavalcante, R. B. L., & Mendes, C. A. B. (2014). Calibração e validação do módulo de correntologia do modelo IPH-A para a Laguna dos Patos (RS/Brasil). *Revista Brasileira de Recursos Hídricos*, 19(3), 191-204. Retrieved in 2022, February 18, from <https://www.abrhydro.org.br/SGCv3/publicacao.php?PUB=1&ID=168&SUMARIO=4793>
- Collischonn, W., Allasia, D., Silva, B. C., & Tucci, C. E. (2007). The MGB-IPH model for large-scale rainfall: runoff modelling. *Hydrological Sciences Journal*, 52(5), 878-895. <http://dx.doi.org/10.1623/hysj.52.5.878>.
- Cunha, A. P., Zeri, M., Leal, K. D., Costa, L., Cuartas, L. A., Marengo, J. A., Tomasella, J., Vieira, R. M., Barbosa, A. A., Cunningham, C., Garcia, J. V. C., Broedel, E., Alvalá, R., & Ribeiro-Neto, G. (2019). Extreme drought events over Brazil from 2011 to 2019. *Atmosphere*, 10(11), 642. <http://dx.doi.org/10.3390/atmos10110642>.
- Diodato, N., Ljungqvist, F. C., & Bellocchi, G. (2019). A millennium-long reconstruction of damaging hydrological events across Italy. *Scientific Reports*, 9(1), 1-10. <http://dx.doi.org/10.1038/s41598-019-46207-7>.
- Diretoria de Hidrografia e Navegação – DHN (2013). Retrieved in 2022, January 20, from <https://www.marinha.mil.br/chm/dados-do-segnav-cartas-raster-347>
- Fan, F. M., & Collischonn, W. (2014). Integração do modelo MGB-IPH com sistema de informação geográfica. *Revista Brasileira de Recursos Hídricos*, 19(1), 243-254. Retrieved in 2019, February 18, from <https://www.abrhydro.org.br/SGCv3/publicacao.php?PUB=1&ID=161&SUMARIO=4350>
- Fan, F. M., Buarque, D. C., Pontes, P. R., & Collischonn, W. (2015a). Um mapa de Unidades de Resposta Hidrológica para a América do Sul. In C. M. A. Alves & M. C. Cunha (Orgs.), *Anais do XXI Simpósio Brasileiro de Recursos Hídricos* (pp. 1-8). Porto Alegre: Associação Brasileira de Recursos Hídricos.
- Fan, F. M., Collischonn, W., Quiroz, K. J., Sorribas, M. V., Buarque, D. C., & Siqueira, V. A. (2015b). Flood forecasting on the Tocantins River using ensemble rainfall forecasts and real-time satellite rainfall estimates. *Journal of Flood Risk Management*, 9, 278-288. <http://dx.doi.org/10.1111/jfr3.12177>.
- Fan, F. M., Siqueira, V. A., Fleischmann, A. S., Brêda, J. P. F., Paiva, R. C. D. D., Pontes, P. R. M., & Collischonn, W. (2021). On the discretization of river networks for large scale hydrologic-

- hydrodynamic models. *Revista Brasileira de Recursos Hídricos*, 26, e5. <http://dx.doi.org/10.1590/2318-0331.262120200070>.
- Fanta, V., Šálek, M., & Sklenicka, P. (2019). How long do floods throughout the millennium remain in the collective memory? *Nature Communications*, 10(1), 1-9.
- Farr, T. G., Rosen, P. A., Caro, E., Crippen, R., Duren, R., Hensley, S., & Alsdorf, D. (2007). The Shuttle Radar Topography Mission. *Reviews of Geophysics*, 45(2), RG2004. <http://dx.doi.org/10.1029/2005RG000183>.
- Fernandes, E. H. L., Marino-Tapia, I., Dyer, K. R., & Möller, O. O. (2004). The attenuation of tidal and subtidal oscillations in the Patos Lagoon estuary. *Ocean Dynamics*, 54(3), 348-359. <http://dx.doi.org/10.1007/s10236-004-0090-y>.
- Fleischmann, A. S., Paiva, R. C. D., Collischonn, W., Siqueira, V. A., Paris, A., Moreira, D. M., Papa, F., Bitar, A. A., Parrons, M., Aires, F., & Garambois, P. A. (2020). Trade-offs between 1-D and 2-D regional river hydrodynamic models. *Water Resources Research*, 56(8), e2019WR026812. <http://dx.doi.org/10.1029/2019WR026812>.
- Fleischmann, A., Siqueira, V., Paris, A., Collischonn, W., Paiva, R., Pontes, P., Crétaux, J.-F., Bergé-Nguyen, M., Biancamaria, S., Gossett, M., Calmant, S., & Tanimoun, B. (2018). Modelling hydrologic and hydrodynamic processes in basins with large semi-arid wetlands. *Journal of Hydrology*, 561, 943-959. <http://dx.doi.org/10.1016/j.jhydrol.2018.04.041>.
- Fox-Rogers, L., Devitt, C., O'Neill, E., Brereton, F., & Clinch, J. P. (2016). Is there really “nothing you can do”? Pathways to enhanced flood-risk preparedness. *Journal of Hydrology*, 543, 330-343.
- Froude, M. J., & Petley, D. N. (2018). Global fatal landslide occurrence from 2004 to 2016. *Natural Hazards and Earth System Sciences*, 18(8), 2161-2181. <http://dx.doi.org/10.5194/nhess-18-2161-2018>.
- Fundação Estadual de Planejamento Metropolitano e Regional – METROPLAN. (2014). Retrieved in 2022, October 13, from http://www.metroplan.rs.gov.br/conteudo/1889/?Estudo_de_alternativas_para_mini
- Fundação Estadual de Planejamento Metropolitano e Regional – METROPLAN. (2017). *Estudos e projeto conceitual de proteção contra cheias do delta do Jacuí em Eldorado do Sul – RS*. Retrieved in 2022, October 13, from https://issuu.com/prefeldoradodosul/docs/revista_tcnica_eldorado_do_sul-c
- G1. (2021). Retrieved in 2022, January 20, from <https://g1.globo.com/rs/rio-grande-do-sul/noticia/2021/11/25/projeto-de-revitalizacao-do-cais-maua-e-apresentado-em-porto-alegre-veja-imagens.ghtml>
- González-Cao, J., Fernández-Nóvoa, D., García-Feal, O., Figueira, J. R., Vaquero, J. M., Trigo, R. M., & Gómez-Gesteira, M. (2021). Reconstrução numérica de cheias históricas extremas: o evento Guadiana de 1876. *Journal of Hydrology*, 599, 126292. <http://dx.doi.org/10.1016/j.jhydrol.2021.126292>.
- Guimaraens, R. (2013). *A enchente de 41*. Porto Alegre: Libretos.
- Jarvis, A., Reuter, H. I., Nelson, A., & Guevara, E. (2008). Retrieved in 2022, October 13, from <http://srtm.csi.cgiar.org>
- Kulman, D., Reis, J. T., Souza, A. C., Pires, C. A. F., & Sausen, T. M. (2014). Ocorrência de estiagem no Rio Grande do Sul no período de 1981 à 2011. *Ciência e Natura*, 36(3), 441-449.
- Lima, A. D. S., Khalid, A., Miesse, T. W., Cassalho, F., Ferreira, C., Scherer, M. E. G., & Bonetti, J. (2020). Hydrodynamic and waves response during storm surges on the southern Brazilian coast: a hindcast study. *Water*, 12(12), 3538.
- Lopes, V. A. R., Fan, F. M., Pontes, P. R. M., Siqueira, V. A., Collischonn, W., & Marques, D. M. (2018). A first integrated modelling of a river-lagoon large-scale hydrological system for forecasting purposes. *Journal of Hydrology*, 565, 177-196. <http://dx.doi.org/10.1016/j.jhydrol.2018.08.011>.
- Machado, A. A., & Calliari, L. J. (2016). Synoptic systems generators of extreme wind in southern Brazil: atmospheric conditions and consequences in the coastal zone. *Journal of Coastal Research*, 75(10075), 1182-1186.
- Magnuszewski, A., & Moran, S. (2015). Vistula River bed erosion processes and their influence on Warsaw’s flood safety. *Proceedings of the International Association of Hydrological Sciences*, 367, 147-154. <http://dx.doi.org/10.5194/piahs-367-147-2015>.
- Martinbianch, G. K., Medeiros, M. S., Fleischmann, A. S., Dornelles, F., Fan, F. M., Paiva, R. C. D. D., Lopes, V. A. R., & Collischonn, W. (2018). Aplicação preliminar do modelo hidrológico MGB-IPH para análise do evento extremo de cheia em 1941 no estado do Rio Grande do Sul. In ABRHidro (Ed.), *Anais do I Encontro Nacional de Desastres* (pp. 1-8). Porto Alegre: Associação Brasileira de Recursos Hídricos. Retrieved in 2019, September 20, from <https://anais.abrhidro.org.br/job.php?Job=3761>
- Martins, J. A., Brand, V. S., Capucim, M. N., Felix, R. R., Martins, L. D., Freitas, E. D., Gonçalves, F. L. T., Hallak, R., Dias, M. A. F. S., & Cecil, D. J. (2017). Climatology of destructive hailstorms in Brazil. *Atmospheric Research*, 184, 126-138.
- Merz, B., Blöschl, G., Vorogushyn, S., Dottori, F., Aerts, J. C., Bates, P., Bertola, M., Kemter, M., Kreibich, H., Lall, U., & Macdonald, E. (2021). Causas, impactos e padrões de enchentes desastrosas. *Nature Reviews Earth & Environment*, 2(9), 592-609. <http://dx.doi.org/10.1038/s43017-021-00195-3>.
- Möller, O. O., Castaing, P., Salomon, J. C., & Lazure, P. (2001). The influence of local and non-local forcing effects on the subtidal circulation of Patos Lagoon. *Estuaries*, 24(2), 297-311. <http://dx.doi.org/10.2307/1352953>.

- Monte, B. E. O., Tschiedel, A. D. F., Silva, D. F., Goldenfum, J. A., & Dornelles, F. (2018). Implicações da ausência de dispositivos de proteção na área urbana de Porto Alegre: análise da cheia de 1941. In ABRHidro (Ed.), *Anais do XII Encontro Anual de Águas Urbanas* (p. 10). Porto Alegre: Associação Brasileira de Recursos Hídricos.
- Müller Neto, J. A., Dornelles, F., Fleischmann, A. S., & Medeiros, M. S. (2019). Estimativa de impacto das cheias de 1941, 1967 e 2015 em Porto Alegre na hipótese de inexistência do sistema de proteção contra cheias do Lago Guaíba. In L. H. Maldonado (Org.), *Anais do XXIII Simpósio Brasileiro de Recursos Hídricos* (p. 10). Foz do Iguaçu: SBRH.
- Nedel, A., Sausen, T. M., & Saito, S. M. (2012). Mapping of natural disasters on Rio Grande do Sul state during 1989 to 2009: hails and wind storms. *Revista Brasileira de Meteorologia*, 27(2), 119-126.
- Oliveira, A. M., Fleischmann, A. S., & Paiva, R. C. D. (2021). On the contribution of remote sensing-based calibration to model hydrological and hydraulic processes in tropical regions. *Journal of Hydrology*, 597, 126184.
- Paiva, R. C., Collischonn, W., & Tucci, C. E. (2011). Large scale hydrologic and hydrodynamic modeling using limited data and a GIS based approach. *Journal of Hydrology*, 406(3-4), 170-181. <http://dx.doi.org/10.1016/j.jhydrol.2011.06.007>.
- Parise, C. K., Calliari, L. J., & Krusche, N. (2009). Extreme storm surges in the south of Brazil: atmospheric conditions and shore erosion. *Brazilian Journal of Oceanography*, 57, 175-188.
- Paz, A. R., Reis, L. G., & Lima, H. V. (2005). Uso de modelagem hidrodinâmica visando a segmentação de corpos d'água rasos para enquadramento: o caso do Lago Guaíba (RS). In ABRHidro (Ed.), *XVI Simpósio Brasileiro de Recursos Hídricos* (pp. 1-20). Porto Alegre: Associação Brasileira de Recursos Hídricos.
- Pontes, P. R. M., Fan, F. M., Fleischmann, A. S., Paiva, R. C. D., Buarque, D. C., Siqueira, V. A., Jardim, P. F., Sorribas, M. V., & Collischonn, W. (2017). MGB-IPH model for hydrological and hydraulic simulation of large floodplain river systems coupled with open-source GIS. *Environmental Modelling & Software*, 94, 1-20. <http://dx.doi.org/10.1016/j.envsoft.2017.03.029>.
- Possa, T. M., Collares, G. L., Boeira, L. D. S., Jardim, P. F., Fan, F. M., & Terra, V. S. S. (2022). Fully coupled hydrological-hydrodynamic modeling of a basin-river-lake transboundary system in southern South America. *Journal of Hydroinformatics*, 24(1), 93-112.
- Pugh, D. T. (1987). *Tides, surges and mean sea-level*. Chichester: John Wiley & Sons.
- Remo, J. W., & Pinter, N. (2007). Retro-modeling the middle Mississippi River. *Journal of Hydrology*, 337(3-4), 421-435. <http://dx.doi.org/10.1016/j.jhydrol.2007.02.008>.
- Remo, J. W., Pinter, N., & Heine, R. (2009). The use of retro-and scenario-modeling to assess effects of 100+ years river of engineering and land-cover change on Middle and Lower Mississippi River flood stages. *Journal of Hydrology*, 376(3-4), 403-416. <http://dx.doi.org/10.1016/j.jhydrol.2009.07.049>.
- Ribeiro Neto, A., Cirilo, J. A., Dantas, C. E. O., & Silva, E. R. (2015). Caracterização da formação de cheias na bacia do rio Una em Pernambuco: simulação hidrológica-hidrodinâmica. *Revista Brasileira de Recursos Hídricos*, 13(3), 47-58. Retrieved in 2022, February 18, from <https://www.abrhidro.org.br/SGCv3/publicacao.php?PUB=1&ID=157&SUMARIO=5064>
- Ridolfi, E., Mondino, E., & Baldassarre, G. (2021). Hydrological risk: modeling flood memory and human proximity to rivers. *Hydrology Research*, 52(1), 241-252.
- Ruhoff, A. L., Paz, A. R., Aragao, L. E. O. C., Mu, Q., Malhi, Y., Collischonn, W., Rocha, H. R., & Running, S. W. (2013). Assessment of the MODIS global evapotranspiration algorithm using eddy covariance measurements and hydrological modelling in the Rio Grande basin. *Hydrological Sciences Journal*, 58(8), 1658-1676.
- Secretaria de Planejamento, Governança e Gestão do Estado do Rio Grande do Sul. (2021). Retrieved in 2022, January 20, from <https://estado.rs.gov.br/estado-apresenta-projeto-de-revitalizacao-do-cais-maua>
- Seiler, L. M., Fernandes, E. H. L., & Siegle, E. (2020). Effect of wind and river discharge on water quality indicators of a coastal lagoon. *Regional Studies in Marine Science*, 40, 101513. <http://dx.doi.org/10.1016/j.rsma.2020.101513>.
- Shuttleworth, W. J. (1993). Evaporation. In D. Maidment (Ed.), *Handbook of hydrology* (pp. 4.1-4.53). New York: McGraw-Hill.
- Sikorska, A. E., Scheidegger, A., Banasik, K., & Rieckermann, J. (2013). Considering rating curve uncertainty in water level predictions. *Hydrology and Earth System Sciences*, 17(11), 4415-4427. <http://dx.doi.org/10.5194/hess-17-4415-2013>.
- Silveira, A. L. L. (2020). Chuvas e vazões da grande enchente de 1941 em Porto Alegre/RS. *Boletim Geográfico do Rio Grande do Sul*, 35, 69-90.
- Siqueira, V. A., Fan, F. M., Paiva, R. C. D., Ramos, M. H., & Collischonn, W. (2020). Potential skill of continental-scale, medium-range ensemble streamflow forecasts for flood prediction in South America. *Journal of Hydrology*, 590, 125430. <http://dx.doi.org/10.1016/j.jhydrol.2020.125430>.
- Siqueira, V. A., Paiva, R. C. D., Fleischmann, A. S., Fan, F. M., Ruhoff, A. L., Pontes, P. R. M., Paris, A., Calmant, S., & Collischonn, W. (2018). Toward continental hydrologic-hydrodynamic modeling in South America. *Hydrology and Earth System Sciences*, 22(9), 4815-4842.

- Smith, M. J., Goodchild, M. F., & Longley, P. (2007). *Geospatial analysis: a comprehensive guide to principles, techniques and software tools*. Market Harborough: Troubador Publishing Ltd.
- Sorribas, M. V., Paiva, R. C., Melack, J. M., Bravo, J. M., Jones, C., Carvalho, L., Beighley, E., Forsberg, B., & Costa, M. H. (2016). Projections of climate change effects on discharge and inundation in the Amazon basin. *Climatic Change*, 136(3), 555-570. <http://dx.doi.org/10.1007/s10584-016-1640-2>.
- Tavora, J., Fernandes, E. H., Thomas, A. C., Weatherbee, R., & Schettini, C. A. (2019). The influence of river discharge and wind on Patos Lagoon, Brazil, suspended particulate matter. *International Journal of Remote Sensing*, 40(12), 4506-4525. <http://dx.doi.org/10.1080/01431161.2019.1569279>.
- Toldo Junior, E., Dillenburg, S., Corrêa, I., Almeida, L., Weschenfelder, J., & Gruber, N. (2006). Sedimentação de longo e curto período na Lagoa dos Patos, Sul do Brasil. *Pesquisas em Geociências*, 33(2), 79-86. <http://dx.doi.org/10.22456/1807-9806.19516>.
- Torres, L. H. (2012). Águas de maio: a enchente de 1941 em Rio Grande. *Historiae*, 3(3), 239-254.
- Trigg, M. A., Wilson, M. D., Bates, P. D., Horritt, M. S., Alsdorf, D. E., Forsberg, B. R., & Vega, M. C. (2009). Amazon flood wave hydraulics. *Journal of Hydrology*, 374(1-2), 92-105.
- Tucci, C. E. (1999). Conflitos do controle de inundação ribeirinha em Porto Alegre. In SBRH (Ed.), *Anais do XIII Simpósio Brasileiro de Recursos Hídricos* (pp. 1-15). Belo Horizonte: SBRH.
- União Europeia – EU. (2007). Directiva 2007/60/CE do Parlamento Europeu e do Conselho, de 23 de outubro de 2007. Dispõe sobre avaliação e gestão dos riscos de inundações. *Jornal Oficial da União Europeia*.
- Valenti, E. D. S. (2010). *Modelo cartográfico digital temático para simulação e previsão de inundações no município de Porto Alegre - RS* (Doctoral dissertation). Centro Estadual de Pesquisa em Sensoriamento Remoto e Meteorologia, Universidade Federal do Rio Grande do Sul, Porto Alegre.
- Valenti, E. D. S., Rolim, S. B. A., & Rocha, R. D. S. (2012). Modelo cartográfico digital temático para simulação e previsão de inundações no município de Porto Alegre – RS. *Revista Brasileira de Cartografia*, 64(3), 331-345. Retrieved in 2022, February 18, from <https://seer.ufu.br/index.php/revistabrasileiracartografia/article/view/43796>
- Vanelli, F. M., Monteiro, L. R., Fan, F. M., & Goldenfum, J. A. (2020). The 1974 Tubarão River flood, Brazil: reconstruction of the catastrophic flood. *Journal of Applied Water Engineering and Research*, 8(3), 231-245. <http://dx.doi.org/10.1080/23249676.2020.1787251>.
- Wongchuig, S. C., Paiva, R. C. D., Siqueira, V., & Collischonn, W. (2019). Hydrological reanalysis across the 20th century: a case study of the Amazon Basin. *Journal of Hydrology*, 570, 755-773. <http://dx.doi.org/10.1016/j.jhydrol.2019.01.025>.
- Yamazaki, D., Sato, T., Kanae, S., Hirabayashi, Y., & Bates, P. D. (2014). Regional flood dynamics in a bifurcating mega delta simulated in a global river model. *Geophysical Research Letters*, 41(9), 3127-3135.
- Zscheischler, J., Westra, S., Van Den Hurk, B. J., Seneviratne, S. I., Ward, P. J., Pitman, A., AghaKouchak, A., Bresch, D. N., Leonard, M., Wahl, T., & Zhang, X. (2018). Future climate risk from compound events. *Nature Climate Change*, 8(6), 469-477. <http://dx.doi.org/10.1038/s41558-018-0156-3>.

Authors contributions

Thais Magalhães Possa: Methodology (writing, figures and preparation of the MGB model for the Patos Lagoon) and Results (writing, model calibration and simulations).

Walter Collischonn: Introduction (writing), general review and editing.

Pedro Frediani Jardim: Methodology (writing, figures and pre-processing of the MGB model) and general review.

Fernando Mainardi Fan: Supervision, general review and editing.

Editor-in-Chief: Adilson Pinheiro

Associated Editor: Ramiro Ignacio Saurral